



UNIVERSITY OF  
BIRMINGHAM

**THE EFFECT OF CRYSTALLINE MORPHOLOGY  
ON THE GLASS TRANSITION AND ENTHALPIC  
RELAXATION IN POLY (ETHER-ETHER-KETONE)**

**MICHAEL TOFT**

A thesis submitted to The University of Birmingham  
for the degree of:

**Masters of Research in the Science and Engineering of Materials**

**Project Supervisor**

**Dr. M. Jenkins**

Department of Metallurgy and Materials  
College of Engineering and Physical Sciences  
The University of Birmingham

September 2011

UNIVERSITY OF  
BIRMINGHAM

**University of Birmingham Research Archive**

**e-theses repository**

This unpublished thesis/dissertation is copyright of the author and/or third parties. The intellectual property rights of the author or third parties in respect of this work are as defined by The Copyright Designs and Patents Act 1988 or as modified by any successor legislation.

Any use made of information contained in this thesis/dissertation must be in accordance with that legislation and must be properly acknowledged. Further distribution or reproduction in any format is prohibited without the permission of the copyright holder.

## Abstract

---

This work investigates the effect of crystalline morphology on the glass transition and ageing characteristics of semi-crystalline PEEK. It is shown that an increasing degree of crystallinity acts to raise the glass transition temperature of the polymer and reduce the overall degree of enthalpic relaxation. For an equal degree of crystallinity the glass transition temperature is also shown to be sensitive to isothermal crystallisation temperature.

By compensating for shifts in  $T_g$  and the influence of crystalline content, samples of varying morphology were produced and physically aged at undercoolings tailored to the  $T_g$  of the system. A greater degree of enthalpic relaxation was observed in cold crystallised samples where the degree of constraint of the amorphous fraction at the crystal/amorphous interface is thought to be greater.

## **Acknowledgements**

---

I would like to thank Dr. Mike Jenkins for his continued advice and guidance throughout this project and Frank Biddlestone for his valuable technical support.

# Contents

---

<b>CHAPTER 1 : INTRODUCTION.....</b>	<b>1</b>
<b>1.1 Synthesis and Properties of Poly(ether-ether-ketone).....</b>	<b>1</b>
<b>1.2 Crystallisation of Polymers.....</b>	<b>3</b>
<b>1.3 The Crystalline Morphology of PEEK.....</b>	<b>5</b>
1.3.1 Origin of Double Melting: Melting and Recrystallisation.....	6
1.3.2 Origin of Double Melting: Primary and Secondary Crystallisation.....	8
<b>1.4 Nature of The Glass Transition, Physical Ageing and Enthalpic Relaxation.....</b>	<b>11</b>
1.4.1 The Glass Transition.....	11
1.4.2 Physical Ageing.....	11
1.4.3 Enthalpic Relaxation.....	12
<b>1.5 The Influence of Crystallinity on the Glass Transition and Enthalpic Relaxation...15</b>	
<b>1.6 Scope of the Work.....</b>	<b>18</b>
<b>CHAPTER 2 : EXPERIMENTAL.....</b>	<b>20</b>
<b>2.1 Materials.....</b>	<b>20</b>
<b>2.2 Differential Scanning Calorimetry (DSC).....</b>	<b>21</b>
2.2.1 Measurements of Crystallinity.....	23
2.2.2 Measurements of Enthalpic Relaxation.....	24
2.2.3 Determination of the Glass Transition Temperature.....	25
<b>2.3 Sample Preparation and Standard Conditioning.....</b>	<b>27</b>

<b>CHAPTER 3 : RESULTS AND DISCUSSION.....</b>	<b>30</b>
<b>3.1 Influence of Cooling Rate on Enthalpic Relaxation in Amorphous PEEK.....</b>	<b>30</b>
3.1.1 Sample Conditioning.....	30
3.1.2 Results and Discussion.....	32
<b>3.2 Influence of Crystallinity on Enthalpic Relaxation.....</b>	<b>34</b>
3.2.1 Sample Conditioning.....	34
3.2.2 Results and Discussion.....	35
<b>3.3 Effect of Crystallinity on the Glass Transition.....</b>	<b>39</b>
3.3.1 Sample Conditioning.....	39
3.3.2 Results and Discussion.....	40
<b>3.4 Effect of Isothermal Crystallisation Temperature on the Glass Transition.....</b>	<b>42</b>
3.4.1 Sample Conditioning.....	42
3.4.2 Results and Discussion.....	45
<b>3.5 Effect of Lamellae Thickness on Enthalpic Relaxation.....</b>	<b>49</b>
3.5.1 Sample Conditioning.....	49
3.5.2 Results and Discussion.....	53
<b>3.6 General Discussion.....</b>	<b>59</b>
<b>CHAPTER 4 : CONCLUSION.....</b>	<b>61</b>
<b>CHAPTER 5 : FUTURE WORK.....</b>	<b>63</b>
<b>REFERENCES.....</b>	<b>65</b>
<b>APPENDIX I : Baseline Subtraction.....</b>	<b>69</b>
<b>APPENDIX II : Formation of Additional Crystallinity on Cooling and Reheating.....</b>	<b>72</b>

## List of Figures

---

<b>FIGURE 1.1</b>	– The Repeat Unit of Poly(ether-ether-ketone).....	1
<b>FIGURE 1.2</b>	– Rate of Crystallisation with Change in Temperature.....	4
<b>FIGURE 1.3</b>	– Peak Crystallisation Times with Temperature for PEEK.....	6
<b>FIGURE 1.4.A</b>	– Deviation of Enthalpy from the Equilibrium Line on Cooling.....	13
<b>FIGURE 1.4.B</b>	– Entalpic Recovery on Tg and Trace for Zero-Ageing.....	13
<b>FIGURE 1.5</b>	– Constrained and Free Amorphous Regions.....	16
<b>FIGURE 2.1</b>	– Trace of Amorphous PEEK Scanned to Melt.....	21
<b>FIGURE 2.2</b>	– Baseline Determination for Calculating Peak Areas.....	23
<b>FIGURE 2.3.A</b>	– Measuring the Glass Transition Temperature.....	26
<b>FIGURE 2.3.B</b>	– Determination of the Glass Transition Temperature in this Work.....	26
<b>FIGURE 3.1.A</b>	– Melting Traces of Amorphous PEEK Cooled Through Tg at Various Rates.....	31
<b>FIGURE 3.1.B</b>	– Glass Transition Region of Amorphous PEEK Cooled Through Tg at Various Rates.....	31
<b>FIGURE 3.2</b>	– Enthalpic Relaxation as a Function of Cooling Rate Through Tg.....	33
<b>FIGURE 3.3.A</b>	– Non-Isothermal Crystallisation Traces at Different Cooling Rates.....	36
<b>FIGURE 3.3.B</b>	– Isothermal Crystallisation Traces at Different Temperatures.....	36
<b>FIGURE 3.4</b>	– Degree of Enthalpic Relaxation for Samples of Various Crystallinities.....	38
<b>FIGURE 3.5</b>	– Broadening of The Glass Transition with Increasing Crystallinity.....	41

<b>FIGURE 3.6</b>	– Glass Transition Temperature as a Function of Crystallinity.....	41
<b>FIGURE 3.7.A</b>	– Cooling PEEK from the Melt to Below Tg at 160 <sup>0</sup> C/min.....	43
<b>FIGURE 3.7.B</b>	– Heating Amorphous PEEK from Below Tg to the Melt at 160 <sup>0</sup> C/min.....	43
<b>FIGURE 3.8</b>	– Double Melting Endotherms of Cold and Melt Crystallised PEEK.....	46
<b>FIGURE 3.9</b>	– Glass Transition Temperature as a Function of Isothermal Crystallisation Temperature.....	48
<b>FIGURE 3.10</b>	– Subtraction of a Sample with Zero Ageing Time from that of an Aged Sample to Calculate Enthalpic Relaxation.....	51
<b>FIGURE 3.11</b>	– Degree of Enthalpic Relaxation for Samples of Equal Crystallinity but Various Lamellae Thickness.....	55



## List of Tables

---

<b>TABLE 2.1</b>	– Mechanical Properties of 450PF PEEK.....	20
<b>TABLE 3.1</b>	– Isothermal Crystallisation Temperatures and Corresponding Times Needed to Control Degree of Crystallinity.....	44
<b>TABLE 3.2.A</b>	– Table of Data for Individual Cold Crystallised Samples with Ageing Times and Temperatures.....	52
<b>TABLE 3.2.B</b>	– Table of Data for Individual Melt Crystallised Samples with Ageing Times and Temperatures.....	52
<b>TABLE 3.3</b>	– Average Data Values for Cold and Melt Crystallised Samples with Measured Tg Onset, End and Breadth.....	57

## Chapter 1 : Introduction

---

### 1.1 Synthesis and Properties of Poly(ether-ether-ketone)

Preparation of the high molecular weight poly(aryletherketone) family by polyether synthesis was first reported by Attwood et al. [1] and the crystalline unit cell of poly(ether-ether-ketone) or PEEK in particular was described by Dawson and Blundell [2] and shown to have the following chemical structure:

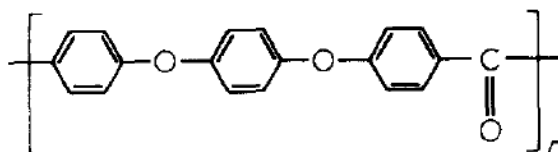


Figure 1.1. The chemical structure of Poly(ether-ether-ketone). [5]

PEEK became commercially available as a high temperature performance thermoplastic, with a glass-transition temperature ( $T_g$ ) of 144°C and a crystalline melting point ( $T_m$ ) of 335°C attributed to the rigid ketone links [2]. The advantage of PEEK over other high temperature polymers at the time, such as poly(ether sulphone), was its degree of crystallinity which improved solvent stress crack resistance and also increased its useful mechanical strength to above 200°C. Despite poly(ether sulphone) having a higher  $T_g$  of 225°C, as the sulphone group prevents crystallinity from developing in the polymer it is amorphous and all mechanical strength is lost around 220°C. The high melting PEEK crystals are able to retain a measurable degree of rigidity in the polymer long after passing through the  $T_g$  and do so until the onset of crystal melting around 300°C [1, 2].

With good mechanical properties, superior chemical resistance and stability at elevated temperatures PEEK soon became recognised as a high-quality engineering thermoplastic [3]. This attracted a great deal of early attention with regards to its morphology and crystallisation kinetics due to its potential use in highly demanding applications [3 – 8]. As a semi-crystalline polymer PEEK also offered relative ease of manufacture as a composite matrix allowing more complex components to be fabricated using conventional polymer processing techniques such as compression and injection moulding, unlike the fibre-reinforced thermosetting polymers [4].

The physical and mechanical properties of semi-crystalline polymers are highly dependent upon their degree of crystallinity, the excellent solvent stress crack resistance of PEEK is not seen unless it is sufficiently crystalline [9, 10]. In addition to this although an increasing degree of crystallinity may slightly improve the tensile properties of PEEK, for the same increase in crystallinity (from 27 to 43%) the mode I fracture toughness of the polymer has been shown to decrease by a factor of almost 3 due to the reduced amorphous content [11].

## 1.2 Crystallisation of Polymers

The crystallisation of polymers can be seen as a dynamic transition from a highly disordered random state, known as the amorphous phase, into ordered three-dimensional spherulites built up from stacks of tightly folded polymer chains, known as lamellae [12]. The crystalline structure of polymers is not a single crystal, but is built up from an array of spherulites. The size, number, structure and perfection of these spherulites depends on the previous thermal history of the polymer and processing conditions such as crystallisation temperature, rate of change of temperature with respect to time, molecular weight of the polymer and any inclusions [12, 13].

As crystals are formed from a highly disordered state, in practise a 100% crystalline polymer is unattainable due to the many entanglements preventing all of the polymer chains arranging into the three-dimensional array required for crystallinity [12]. Therefore polymers which are able to develop a certain degree of crystallinity are known to be semi-crystalline. As a semi-crystalline polymer, PEEK can be obtained in either an amorphous or crystalline form as a direct result of the processing conditions from the melt. A glassy or amorphous state is achieved by rapidly quenching from the melt to below  $T_g$ , whereas slow cooling the melt will allow crystallinity to develop in the sample (melt crystallisation) [5]. The crystalline form can also be obtained on heating the glass through the  $T_g$  (cold crystallisation) or by holding the polymer at a constant temperature between  $T_g$  and  $M_p(^{\circ}C)$  for a given length of time (isothermal crystallisation) [3, 4].

As crystallisation and melting are thermodynamically driven, in order for phase transformations to take place there must be a favourable change of the energy in a system [14, 15]. On crystallisation when cooling from the melt in order to accommodate the change in temperature it is favourable for the disordered amorphous state of high molecular mobility to arrange into a much more ordered state of lower energy, resulting in a large negative energy contribution (i.e. the crystallisation exotherm) [12, 14]. On reheating this crystalline structure into the melt an increase in the energy of the system no longer favours ordered structures and the absorption of energy results in melting of the crystals and mobilisation of the amorphous phase (i.e. the melting endotherm) [12, 14].

Polymer crystallisation can be broken down into a series of events. Initially the nucleation barrier must be overcome, where intramolecular forces order chains to form a stable nucleus. Growth of the crystalline region then occurs as additional chains are aligned at the growing crystal face and long range order is seen as a regular three-dimensional structure is developed [12, 14]. Growing crystals may then impinge on neighbouring crystals and should conditions permit, rearrangements within the crystalline structure can be seen known as crystal perfection [14].

However due to the complex nature of crystallisation, in practical situations nucleation and growth occur at different points and may proceed at different rates giving a distribution in the size and perfection of crystallites. As shown in Figure 1.2 crystallisation rate is highly dependent on temperature and is restricted to a range of temperatures between the  $T_g$  and  $T_m$  of the polymer.

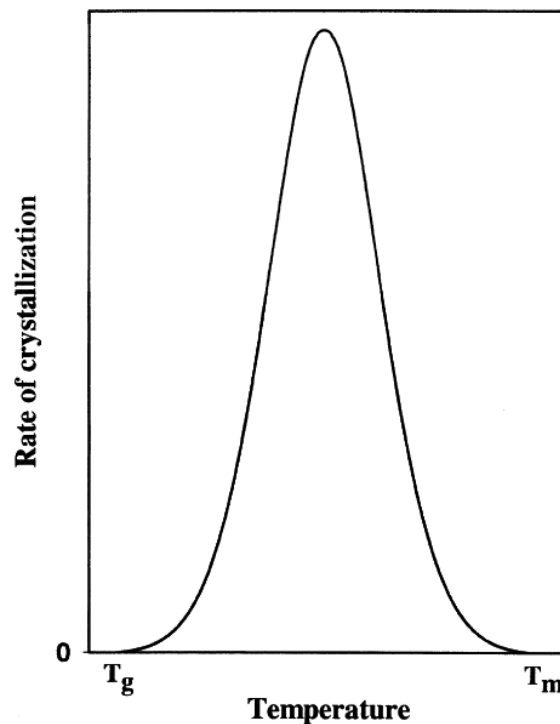


Figure 1.2. Dependence of crystallisation rate on temperature. [15]

At temperatures above  $T_m$  there is a great deal of energy in the system and the segmental motion of the polymer chains is too great for stable nuclei to form and for crystalline growth to occur [12,15]. However as the temperature is reduced below  $T_m$  there is an increase in melt viscosity and therefore an increased opportunity for nucleation to occur, growing a microstructure of few but very large crystals. As the temperature is further reduced and viscosity increases the rate of crystallisation passes through a maximum where conditions favour both nucleation and growth of crystallites [12].

On approaching  $T_g$  there is much less energy in the system and the molecular motion of the polymer chains is greatly reduced. In such a viscous state there is a much lower nucleation barrier opposing the formation of stable nuclei, however due to low molecular mobility transport of the chains to the crystal growth front is hindered [15]. This gives a microstructure with a greater number of crystallites but considerably smaller in size. Below  $T_g$  the polymer chains are in effect 'frozen' in position and no further crystallisation can take place [16, 17].

### **1.3 The Crystalline Morphology of PEEK**

The first work investigating the morphology of PEEK was done by Blundell and Osborn [5] who noted that in their system the maximum rate of crystallisation occurred around 230°C as shown in Figure 1.3. However this is subject to the molecular weight of the polymer which determines factors such as the onset of crystallisation and crystallisation rates [13]. The upper, melt crystallised, data points were obtained by melting the polymer at 400°C for 2 minutes to erase any previous thermal history and then rapidly cooling to the crystallisation temperature ( $T_c$ ) for a crystallisation time ( $t_c$ ) and recording the peak time of the crystallisation process. The lower, cold crystallised, data points were obtained by quenching the polymer in liquid nitrogen directly from the melt to form an amorphous glassy state before rapidly heating to  $T_c$  for  $t_c$  and again recording the peak crystallisation time.

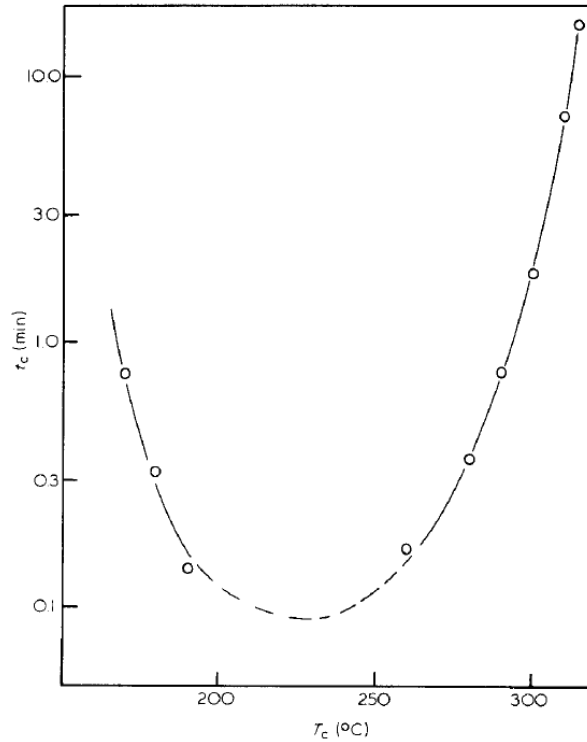


Figure 1.3. Variation in peak crystallisation times for samples isothermally crystallised at different temperatures. [5]

On scanning samples that had been isothermally crystallised at a range of different temperatures an interesting phenomenon was observed, known as double melting. When reheating the samples to the melt a trace was produced with a first low temperature melting peak (or endotherm) that appeared  $\sim 10^\circ\text{C}$  above the original isothermal crystallisation temperature and a second high temperature endotherm, much larger in magnitude. The second, upper melting peak was found to occur  $\sim 335^\circ\text{C}$  regardless of isothermal temperature (being slightly higher for samples crystallised at a higher  $T_c$ ).

### 1.3.1. Origin of Double Melting: Melting and Recrystallisation

Due to the similarity of PEEK's main thermal transitions with those of poly(ethylene terephthalate) (PET), Blundell and Osborn [5] drew upon the well documented behaviour of PET when considering PEEK's crystalline morphology. In particular the double melting traces seen for PEEK were comparable to those produced by Holdsworth and Turner-Jones [18] who cold crystallised PET at

various temperatures and times before cooling and rescanning. The phenomenon of double melting seen in PEEK by Blundell and Osborn was described as the effect of a continuous melting and recrystallisation process that takes place during the scan [5, 18].

The DSC heating scan of amorphous PET first shows a large and broad exothermic crystallisation peak, indicating that a range of crystalline entities with a varying degree of crystal perfection are formed. Between this exothermic peak and the endothermic melting peak there is a wide intermediate temperature range, in which there is no detectable change in the DSC baseline. However it was reported that on several samples the area under the melting peak was 20-30% greater than that of the crystallisation peak [18]. With support from x-ray data they proposed that the increase in crystallinity is due to an increase in the average perfection of the crystallites, developed over the intermediate temperature range.

During a DSC heating scan the temperature is continuously increasing. It is postulated that for a given temperature over the intermediate range the least perfect crystals at that time will experience melting and will recrystallise to form more perfect crystals later in the scan. At that same time previously less perfect crystals that have already melted, will undergo recrystallisation to form more perfect crystals. More perfect, stable crystals will not experience melting or recrystallisation until a high enough temperature is reached. There is no net movement of heat and therefore no detectable change in the DSC baseline, despite an overall increase in the average perfection of the crystal population. The broad endothermic melting peak represents the point where the temperature is too high for recrystallisation of melting crystals, with a distribution of size and perfection [5, 18].

Both Holdsworth and Turner-Jones along with Blundell and Osborn propose that the double melting seen on DSC traces is not representative of the polymer morphology present at room temperature before scanning. They argue that it is the first, low temperature endotherm which is to be associated with the crystals formed during the thermal treatment, whereas the second, upper endotherm is a characteristic of the polymer system and due to the melting and recrystallisation process [5, 6, 18]. This is in concurrence with their results and explains why the first peak is found to be slightly above



the treatment temperature and also why the second peaks are found at a much more definite temperature.

If the DSC heating scan is stopped and the system is cooled at a point along the intermediate temperature range, then the continuous melting and recrystallisation procedure will be suspended. This will leave a population of crystals that have previously melted and recrystallised to form more perfect crystals, with a higher melting temperature. On rescanning these crystals melt at a slightly higher temperature than the treatment temperature, producing the first endotherm before the equilibrium between continuous melting and recrystallisation processes is re-established [18]. As the treatment temperature increases and approaches the melting point of the polymer, the recrystallisation of melted crystals will be prevented and the process will be reduced until only a single peak is observed representing the original thermal treatment.

It is made clear that the melting and recrystallisation process may only occur in a small portion of the crystallites and that the whole of the crystal does not necessarily have to melt before recrystallisation can take place [18]. A distinction is also made between the upper melting peak, where the melting process passes through a maximum ( $\sim 335^{\circ}\text{C}$ ), and the thermodynamic melting point for an infinitely large crystal which is estimated to be  $395^{\circ}\text{C}$  for PEEK [5].

### **1.3.2 Origin of Double Melting: Primary and Secondary Crystallisation**

However the theory that continuous melting and recrystallisation produced the double melting endotherms in heat treated PEEK became an area of discontent in the literature. Other authors at the time argued that the double melting peaks were representative of two crystal morphologies formed at different times during the thermal treatment [3, 4, 7, 8]. They do not support the idea that all the crystals formed at the treatment temperature are represented by the first endothermic peak and that the second upper peak is purely associated with melting and reorganisation of these crystals. It is argued that the area under the first peak is too small to account for the melting of the whole crystalline

fraction formed at a given treatment temperature [3, 4]. Instead they hypothesised that for a given treatment temperature imperfect, unstable crystals may form between existing lamellae and then melt when heated above this formation temperature, resulting in the lower and upper endotherms.

In particular work done by Bassett et al. [7] using permanganic etching led the authors to argue that double melting is due to the morphological sitting of two distinct components of crystallinity formed during separate stages of crystallisation. They propose that the upper melting peak is representative of a framework of primary lamellae which form in an unrestricted environment to occupy the available space but not to fill it. The material represented by the lower melting peak then forms in less available space and a more restricted environment between these primary lamellae. The orientations and conformations may be predetermined to some degree by molecules along the chain which may already be entangled in the first lamellae, reducing the stability of these secondary crystals [7]. Thus, on annealing at increasingly higher temperatures these less stable crystals melt and recrystallise with an increasingly higher lamellae thickness which will now melt slightly above the annealing temperature. Also on isothermally crystallising for longer periods of time they are able to develop more fully, giving rise to the increasing prominence of the lower temperature, secondary peak with annealing time.

The authors in support of two separate crystal morphologies being the cause of double melting do not dispute the possibility of modest reorganisation of crystallites on slow heating. It is the origin of the upper melting peak that is felt to originate from a primary crystal population present at room temperature, as opposed to coming from a complete reorganisation of the lower temperature endotherm.

The work presented herein supports the hypothesis of a dual lamellae morphology, with the formation of a secondary population of crystallites between the initially formed primary crystals on holding for prolonged periods of time at a given isothermal temperature. The secondary crystallites which form between the primary population are represented by the lower and upper endotherms respectively. It is felt that the heat of fusion on melting, as measured from the low temperature endotherm, is too small

to account for the total degree of crystallinity developed on crystallisation at a given isothermal temperature. However it is important to note this work does not dispute the fact that when using slow scanning rates melting and recrystallisation can be observed [Appendix I & II].

## **1.4 Nature of The Glass Transition, Physical Ageing and Enthalpic Relaxation**

### **1.4.1 The Glass Transition**

The glass transition temperature ( $T_g$ ) refers to the dynamic transformation of a non-crystalline solid from a liquid to a glassy state or vice versa and in particular describes this change of state for the amorphous phase of a polymer (whether semi-crystalline or not). On cooling through  $T_g$  the glass is no longer able to remain in a state of structural equilibrium within a finite time scale and thus falls into a metastable state [16, 17]. Such a structure becomes ‘frozen in’ as on cooling at a given rate from equilibrium above the  $T_g$ , the packing of amorphous molecular chains needed to accommodate the change in temperature is made impossible by the time-scale imposed by the rate of cooling. It therefore follows that a faster cooling rate would cause the system to deviate further from the equilibrium and if stored at sufficiently low temperatures below  $T_g$  it would effectively remain in this state with excess thermodynamic quantities such as volume and enthalpy for an infinite length of time [19, 20, 21].

However if the polymer is held at temperatures approaching  $T_g$  the glass undergoes relaxation towards its thermodynamic equilibrium with a reduction of excess volume and enthalpy, although there is only a small temperature range in which such relaxation can be realistically observed. As the ageing temperature ( $T_a$ ) (i.e. the temperature the glass is held below  $T_g$ ) increases, the length of time it takes for the system to approach equilibrium is vastly increased and it is often not possible to reach equilibrium further than 15°C below the  $T_g$  of a polymer [19]. It is common for ageing experiments to take place at reasonably small undercoolings from the measured  $T_g$ , so that experimental results can be obtained in an acceptable time frame.

### **1.4.2 Physical Ageing**

The term physical ageing is used to describe the volume relaxation and enthalpy relaxation which occurs as the glass approaches a more stable state of equilibrium and causes a change in the mechanical properties of the polymer. It is important to note that physical ageing refers to reversible

changes in polymer properties, unlike chemical ageing which is associated with processes such as degradation or breakage of bonds [20].

When stored at temperatures approaching but below  $T_g$  for a given time, physical ageing has been shown to affect the mechanical properties of polymers. Yield stress has been shown to increase with ageing time, indicating that more mechanical work is needed to deform the specimen to recover the degree of enthalpy lost on ageing [22]. Although increases in yield stress are seen with ageing, a marked decrease in impact strength has also been shown, indicating that the material becomes much more brittle [22]. Similar increases in tensile yield stress, with more localised yielding, along with a decrease in impact strength have been shown to occur on ageing amorphous PEEK samples [23]. Due to the influence of physical ageing on the mechanical properties of polymers it is important to understand the mechanisms behind ageing, this can be done experimentally using techniques to investigate manifestations of ageing such as enthalpic relaxation.

### **1.4.3 Enthalpic Relaxation**

Although dilatometry can be used to measure the volume relaxation associated with physical ageing, calorimetric studies are considerably more common and in particular differential scanning calorimetry can be used to determine enthalpic relaxation on ageing. As DSC is the technique adopted in this work the discussion shall focus solely on enthalpy relaxation and although it is analogous to volume relaxation as determined by dilatometry, differences between the two techniques must be stressed [19]. The concept of enthalpic relaxation on ageing and its subsequent recovery as an endothermic peak on a DSC trace is best represented schematically, Figure 1.4.

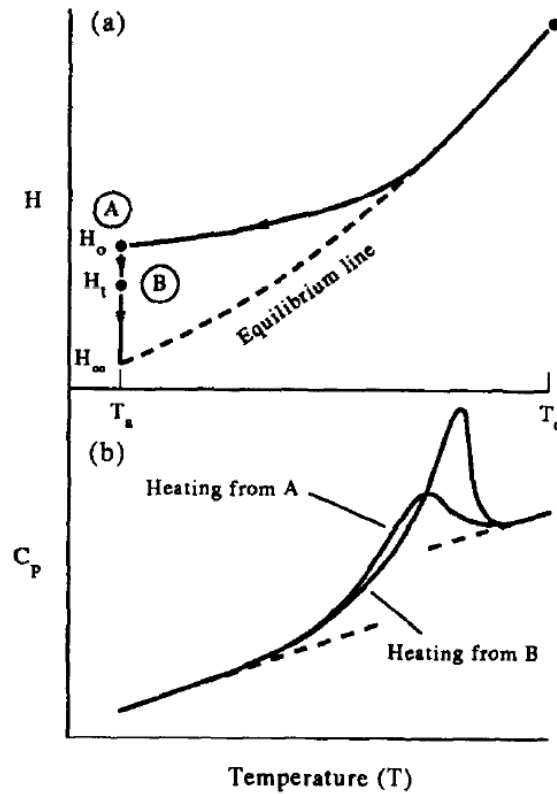


Figure 1.4. a) Enthalpy as a function of temperature. On cooling at a constant rate from equilibrium at  $T_0$ , state A is obtained; after ageing at  $T_a$  for time  $t$  the system reaches state B with an enthalpy relaxation of  $H_t$  as it moves towards the enthalpy equilibrium  $H_\infty$ . b) Specific heat as a function of temperature. Trace B is recorded first and shows the enthalpy recovered on heating through  $T_g$  before the sample is cooled at the same rate back to A and scanned for zero ageing time. [19]

On cooling from the liquid state to the glass the amorphous material can be seen to deviate from the equilibrium line at  $T_g$  and proceed to point A in Figure 1.4.a. On ageing the system at temperature  $T_a$  there is a driving force towards the thermodynamic equilibrium  $H_\infty$  and a corresponding reduction in enthalpy. If the system is then aged for time,  $t$ , it will have been reduced to the value  $H_t$  at point B. The loss in enthalpy between point A and B, or enthalpic relaxation, is then recovered as an endothermic peak on the DSC traces between  $T_a$  and  $T_0$  as seen in Figure 1.4.b. Trace B is taken first and is that of the aged sample (from point B), as seen by the much more pronounced enthalpic peak on  $T_g$ . Trace A is recorded by rescanning the sample for zero ageing time (from point A) as on heating trace B above  $T_g$  to  $T_0$  equilibrium is restored and the previous enthalpic relaxation is erased.

This gives two traces which can then be superimposed so that the trace of the sample for zero ageing time can be subtracted from that of the sample aged at temperature  $T_a$  for time  $t_a$ . Integration of the resultant area after subtraction must then be performed to determine the enthalpic relaxation, or physical ageing of the sample, between points A and B [19, 20, 21]. If  $T_a$  is moved to increasingly higher temperatures the rate at which the system is able to relax increases, although as can be seen from Figure 1.4.a as it has deviated less from the equilibrium line the overall degree of relaxation possible ( $H_\infty$ ) will be reduced.

## 1.5 The Influence of Crystallinity on the Glass Transition and Enthalpic Relaxation

Although  $T_g$  and enthalpic relaxation are associated with the amorphous phase of the polymer, in semi-crystalline structures the crystalline phase (which is already in a state of equilibrium as it is cooled through  $T_g$ ) has been shown to influence the nature of the glass transition and also the degree of enthalpic relaxation on physical ageing. Therefore the traditional two-phase model of semi-crystalline polymers consisting only of a crystalline and an amorphous fraction could no longer be used to describe this effect. It became evident that molecular interactions at the crystal/amorphous interface could be used to describe such effects and consequently work was done to investigate the morphology of this intermediate region.

A new model for semi-crystalline polymers was first introduced in a series of papers by Struik [24 – 27] whereby crystals disturb the amorphous phase and reduce their segmental mobility, giving the amorphous phase a  $T_g$  distribution. Amorphous regions adjacent to the crystal surface will experience the greatest degree of restriction, with the effect reducing as you progress through the interface and reach the amorphous phase unrestricted by crystallites and with properties equal to those of the bulk amorphous material [24, 25].

A similar interpretation of the crystal/amorphous interface led to the development of a three-phase model consisting of the crystalline phase, a rigid amorphous fraction (RAF) and a mobile amorphous fraction (MAF) [28, 29, 30]. Due to the highly entangled nature of polymer systems, on crystallisation and cooling below  $T_g$  amorphous layers which are unable to crystallise themselves become entwined with crystalline regions and are constrained in loops and chains connected to the crystal surface [30]. This is described as the RAF [Figure 1.5], however the physical tethering of amorphous chains progressively decreases as you move away from the crystal surface, giving the amorphous fraction an increasingly greater degree of mobility. The MAF relates to the unconstrained bulk amorphous phase, which exhibits the sharp liquid to glass transition at  $T_g$  as described earlier [30]. For clarity, this work shall refer to restrictions at the crystal/amorphous interface and the bulk amorphous regions as the constrained amorphous region and the free amorphous region respectively.



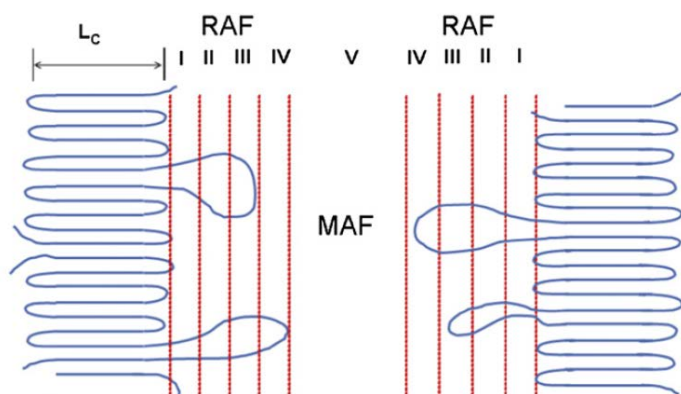


Figure 1.5. Representation of the constrained amorphous region (RAF) in close proximity to the crystal lamellae in comparison to the free amorphous region (MAF) at distances further from the interface. [adapted from 30]

This constraint at the crystal/amorphous interface has been shown to have a marked effect on the  $T_g$  of a semi-crystalline polymer when compared to that of its fully amorphous counterpart [31]. As crystallinity is introduced the position of  $T_g$  is shifted upwards, and also due to the progressive increase in mobility of the constrained amorphous regions with an increase in temperature the breadth of the transition is considerably increased [31, 32, 33]. The size of the step change at  $T_g$  ( $\Delta C_p$ ) is also reduced due to segmental constraints of the amorphous regions, as there is a decrease in the number of main chain rotational modes which are able to activate at the transition [31, 32].

The introduction of crystallinity into a polymer system not only increases the breadth and measured position of the glass transition temperature, but has also been shown to reduce the overall degree of physical ageing. For example the enthalpic relaxation of semi-crystalline poly(ethylene terephthalate) (PET) was found to be considerably lower than that of its fully amorphous counterpart for an equal  $T_a$  and  $t_a$  [34]. Although a reduction in enthalpic relaxation may be expected due to a reduced amorphous content, the ageing effects in semi-crystalline PET could not only be described using a two-phase model and it became evident that crystallites reduced segmental mobility of the amorphous phase [34, 35]. Work on other semi-crystalline polymers including polypropylene (PP) [36] and PEEK [32] has also shown that segmental mobility of the amorphous fraction is restricted at the crystal/amorphous interface and consequently influences the physical ageing characteristics of the polymer.

Although work has been done investigating the effect of crystallinity on the glass transition temperature and enthalpic relaxation characteristics separately, the two have not been studied in parallel. As enthalpic relaxation is highly dependent on the degree of undercooling below  $T_g$  [19], any influence of restriction at the crystal/amorphous interface on the glass transition will therefore have an effect on ageing kinetics. In addition to this variations in crystalline morphology and the degree of constrained amorphous regions will also contribute to the glass transition and enthalpic relaxation characteristics, no such work has been done correlating these effects.

## 1.6 Scope of the Work

The purpose of this work is to investigate the effect of crystalline morphology on the glass transition temperature and degree of enthalpic relaxation seen in poly(ether-ether-ketone). Due to the use of PEEK as a high performance engineering thermoplastic, often at above ambient temperatures, how the morphology of the polymer influences its response to physical ageing is of particular commercial interest.

During the processing of PEEK using techniques such as compression or injection moulding, the polymer is often quenched from the melt to temperatures below  $T_g$  leaving the amorphous phase in a state far from equilibrium. As outlined above, if the service temperature approaches  $T_g$  this will cause physical ageing and a change in material properties over time. If by altering the morphology you are able to reduce the amount of physical ageing seen over a period of time at a given temperature this would be of considerable benefit to the user.

The main focus of this work is to engineer two distinct crystal morphologies into the polymer by melt crystallising and cold crystallising samples to produce a population of few but large, and many but small crystallites respectively. It is important to note that the degree of crystallinity in the melt and cold crystallised samples will be controlled, so that it will be the distribution of lamellae (i.e. crystallite size) that will influence enthalpic relaxation as opposed to variations in the amount of amorphous material present.

The originality of this work in particular is to compensate for the shift in  $T_g$ 's with change in crystallite size. Therefore if the  $T_g$  is calculated for a given population of lamellae crystals by using the same degree of undercooling ( $\Delta T$ ) the samples will be aged at a temperature tailored to the individual morphology of the system as:  $T_g - \Delta T = T_a$ .

This is essential because if the  $T_g$  shift is not accounted for, as is often the case, and  $T_a$  remains the same you are essentially measuring the effect of altering  $\Delta T$ . As described in section 1.4.3 the further you age below  $T_g$  the slower the relaxation kinetics are, along with a greater possible degree of enthalpic relaxation towards  $H_\infty$ , up to a point around 15°C below  $T_g$  where relaxation cannot be

measured on a finite time scale. By tailoring the ageing temperature to the system you are able to avoid this problem and for samples of equal crystallinity, could therefore investigate how the enthalpic relaxation is affected by the constraint of an identical amount of amorphous material between different crystal morphologies.

## Chapter 2 : Experimental

---

### 2.1 Materials

The material used in this study was poly(ether-ether-ketone), as supplied by Victrex in the form of a semi-crystalline fine powder (450 PF) with the following material properties as given in supplementary data sheets which can be found at [victrex.com](http://victrex.com):

**Table 2.1: Typical Values for selected properties of 450PF PEEK**

<b>Material Property</b>	<b>Units</b>	<b>450PF</b>
Tensile Strength (23°C)	MPa	100
Tensile Modulus (23°C)	GPa	3.7
Izod Impact Strength (Notched 23°C)	kJm <sup>-2</sup>	6.5
Glass Transition (Onset)	°C	143
Melting Point	°C	343

## 2.2 Differential Scanning Calorimetry

Differential scanning calorimetry (DSC) is a technique whereby the temperature and power output to a sample and reference cell are continuously monitored as they are simultaneously heated and cooled (non-isothermal) or held (isothermal) at identical temperatures. Therefore any variation in temperature that occurs between the sample and reference cell is due to a thermal transition in the polymer sample. The differential technique is used to assess this heat flow and equalise the incident heat gains or losses between the two cells by increasing or decreasing the power output to the sample cell as required [37, 38]. This change in output (mW) can be monitored in order to determine the heat flow into or out of the system and plotted with respect to change in temperature for non-isothermal studies or change in time for isothermal studies [14, 37, 38].

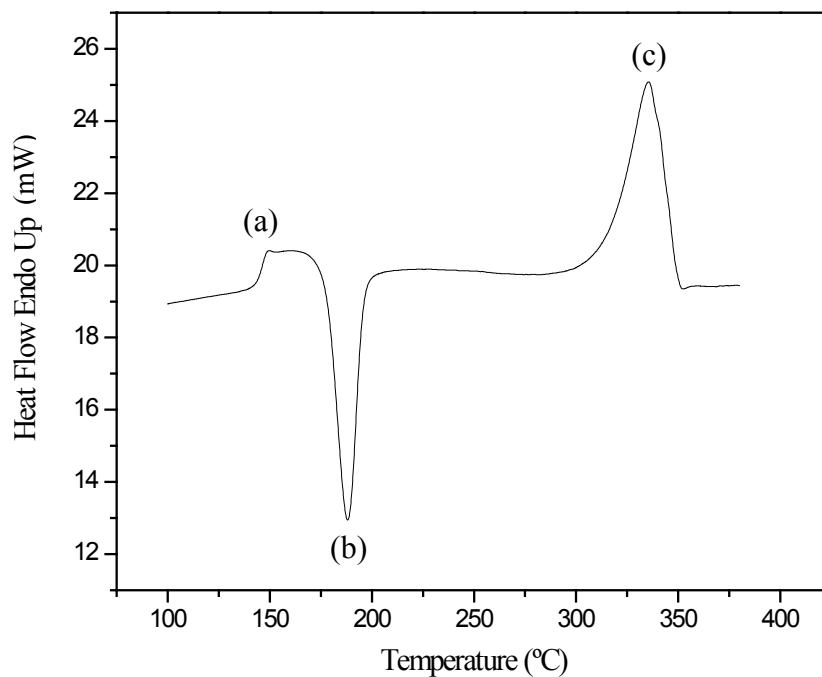


Figure 2.1. DSC trace of amorphous 450PF PEEK scanned from below  $T_g$  into the melt exhibiting a)  $T_g$  step b) crystallisation exotherm c) melting endotherm.

Figure 2.1 is a DSC trace obtained on scanning amorphous 450PF PEEK into the melt and shows the thermal transitions in the order (a) glass transition, (b) crystallisation dip and (c) crystal melting peak as the polymer is heated from below  $T_g$  into the melt. As the sample absorbs energy, in the case of  $T_g$  or the melting of crystallites, there is an increase in heat flow to the sample needed to mobilise molecular chains which can be described as an endothermic process. On the other hand as the liquid-like phase moves to a state of lower entropy (crystallisation) there is an output of heat from the polymer and a resulting decrease in the heat flow to the sample, known as an exothermic process.

Due to the sensitivity of a calorimeter, in order to obtain accurate results there are a number of factors which must be taken into account to improve the reproducibility of conditions between samples. To begin with the packing of the sample in the pan is important as this determines the degree of thermal contact between the sample/pan and ultimately the contact with the sensor [39]. The amount of sample used is also of importance and in order to maintain the sensitivity of the instrument only a limited range of sample masses are appropriate. If the sample is too thick then a temperature gradient may be set up and cause the comparatively cool upper surface, located further from the heating element, to lag behind that of the hotter base [39, 40]. At increasingly higher scanning rates thermal lag inherent to DSC has also been shown to broaden sample response so should be taken into account [40]. Finally due to small sample sizes even the position of the pans inside the DSC cells should be considered, locating them as centrally as possible to reduce any anomalous effects that may be introduced by the slight temperature gradient (tenths of a degree) between the centre and outer edge of the cell [39].

Care should not only be taken during the preparation of samples and running of the DSC but also on the interpretation and analysis of the traces produced in order for results to be comparable, as discussed in the following sections.

### 2.2.1 Measurements of Crystallinity

In order to calculate the degree of crystallinity of a semi-crystalline polymer sample the area under the melting peak, or the heat of fusion ( $\Delta H_f$ ), must first be measured. However due to the distribution of lamellae and crystallite sizes within a polymer, melting may take place over a wide temperature range making it difficult to determine the onset of crystal melting [41, 42, 43]. As shown in Figure 2.2, drawing an arbitrary baseline under the melting peak thus becomes a very subjective operation and any instrumental baseline slope or curvature may significantly alter the estimate of the shape or extent of the baseline to be drawn [41].

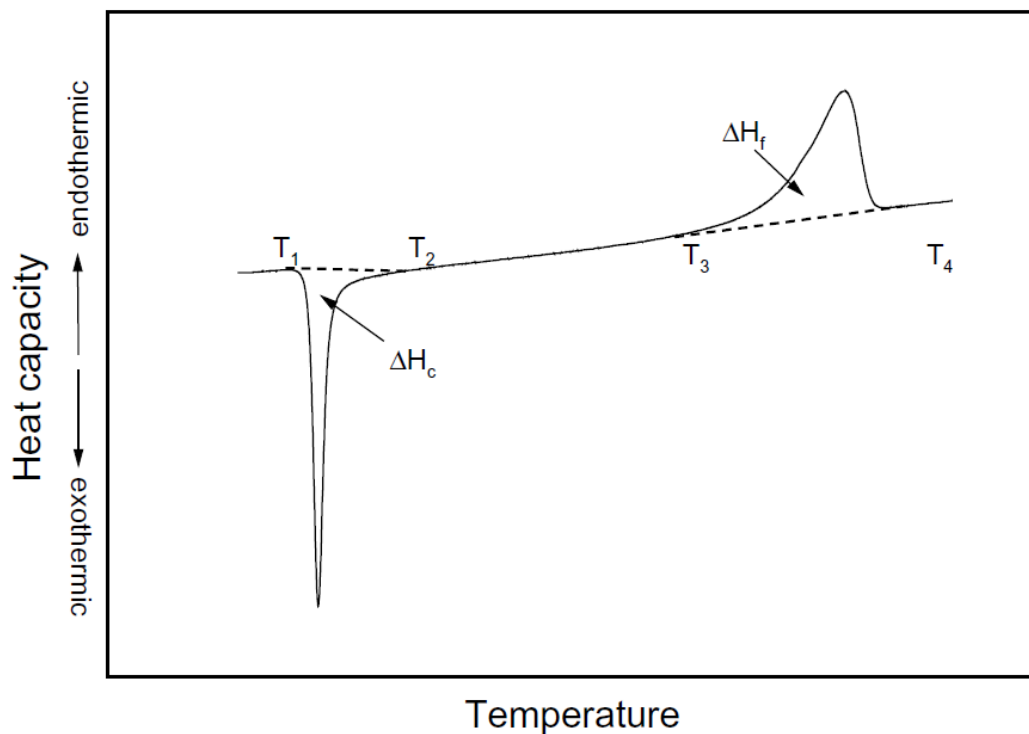


Figure 2.2. Measurements of the crystallisation exotherm and melting endotherm using arbitrarily drawn baselines between T<sub>1</sub>-T<sub>2</sub> and T<sub>3</sub>-T<sub>4</sub> respectively. [44]



Methods have been proposed in order to overcome such difficulties whereby the baseline of an empty pan could be subtracted from the sample trace [41, 42]. However such a procedure did not improve data sets in this work so was not adopted. As shown in Appendix I measurements made on features of the melting endotherm were consistent amongst themselves allowing for an accurate heat of fusion to be determined.

The enthalpy of fusion ( $\Delta H_f$ ) for the area measured under the melting peak must then be divided by the theoretical enthalpy of fusion for fully crystalline PEEK ( $\Delta H_{fc}$ ), taken to be 130 J/g [5] so the degree of crystallinity ( $X_c$ ) of the sample can be determined. Despite the importance of the crystal/amorphous interface when interpreting polymer morphology, the two-phase model is adequate when taking physical measurements such as the weight fraction of crystalline ( $x$ ) and amorphous ( $1 - x$ ) material [5].

$$X_c (\%) = \frac{\Delta H_f (\text{J/g})}{\Delta H_{fc} (\text{J/g})} \quad (\times 100)$$

### **2.2.2 Measurements of Enthalpic Relaxation**

To measure the degree of enthalpy lost on ageing and recovered as an endotherm on reheating through the glass transition, the trace of the un-aged sample must be subtracted from that of the aged sample and the resulting area integrated. As shown previously in Figure 1.4.b, in order to obtain accurate results the glassy and liquid regimes of the two curves must superimpose before and after  $T_g$  respectively, so that only the enthalpy recovered from ageing is measured.

Superposability can be achieved by re-scanning the sample for zero ageing time immediately after the trace of the aged state has been recorded by heating to a temperature above  $T_g$  and cooling back to the starting temperature at a constant rate [19, 20, 21]. This prevents the introduction of any anomalies

into the system from things such as temperature/calibration drift, location of the sample in the cell, variations in baseline or differences between samples [39]. In order to eliminate any effects of thermal inertia it is also common practice to cool the sample from the ageing temperature down to some lower temperature and begin the scan from there [20]. Due to the use of finite heating rates and the increasingly long time scales needed for relaxation as you cool further below  $T_g$  to this lower temperature, no further enthalpic relaxation is able to take place.

### **2.2.3 Determination of the Glass Transition Temperature**

Due to the complex nature of the glass-transition and its dependence on things such as the rate at which the polymer is cooled from equilibrium, additional restriction of molecular mobility from the presence of crystallites and subsequent annealing, interpretation of the DSC trace can be difficult [45, 46, 47]. Therefore in order to determine a meaningful and accurate measure of  $T_g$  it is important to carefully control experimental conditions such as the heating and cooling rate, especially as the transition is strongly rate dependent and the DSC is a dynamic instrument [45].

As shown in Figure 2.3.a. an accurate value of  $T_g$  can be measured at the mid-point of the sigmoidal change in heat capacity where lines from the glass and liquid phases which lie outside the transition region can be extrapolated to intersect. The method adopted when defining a glass-transition temperature on heating from the glassy to the liquid phase in this work is shown in Figure 2.3.b. where the midpoint of the glass-liquid transition is calculated using Pyris software. As measurements were not taken on samples with an endothermic relaxation peak on  $T_g$  [45], and were instead taken on the corresponding trace for zero-ageing time, this method is accurate.

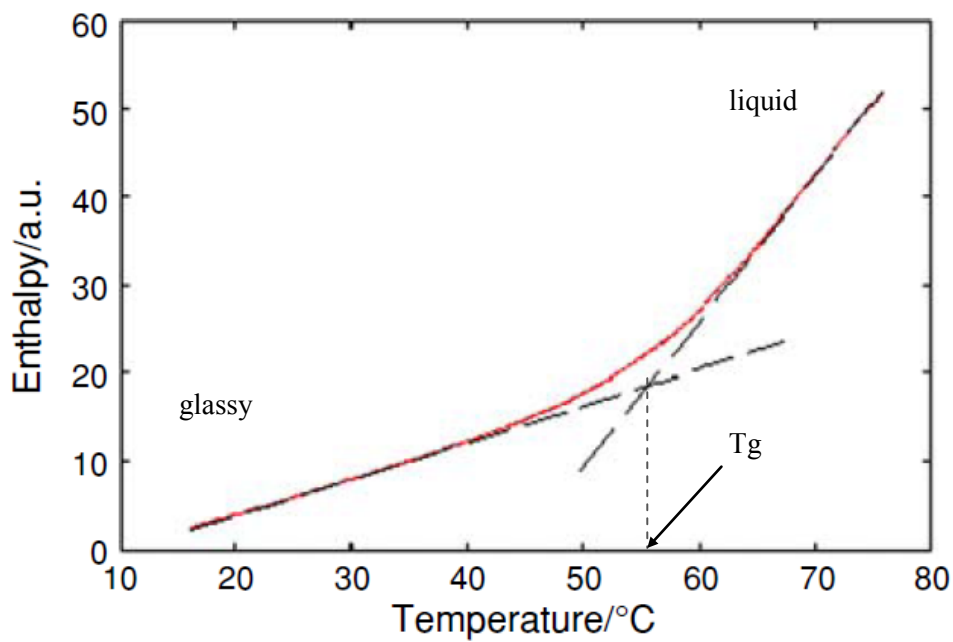


Figure 2.3.a. Determination of  $T_g$  at the interception of lines extrapolated from the liquid and glassy states. [adapted from 47]

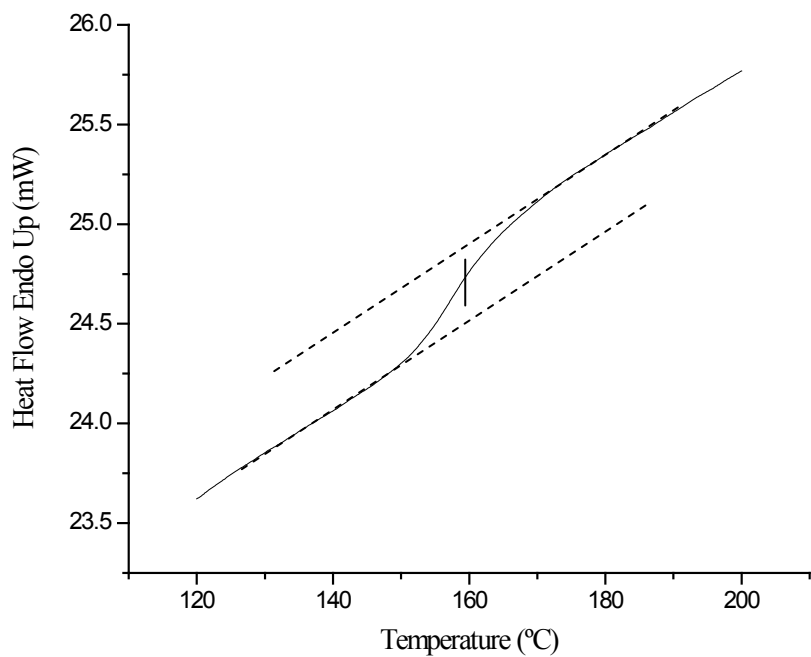


Figure 2.3.b. Method of calculating  $T_g$  as used in this work.

### 2.3 Sample Preparation and Standard Conditioning

In this study a power compensated Perkin-Elmer DSC7 was used and interfaced to a computer for data acquisition and analysis using Pyris and Origin software. A sample mass of 5.25 mg ( $\pm$ ) 0.05mg was used to ensure good coverage over the base of the Al sample pan for improved sample/pan contact yet remain thin enough to prevent the establishment of any significant thermal gradient. The sample was encapsulated in the pan in order to prevent spillage of the powder and also to give a constant emissivity between samples by reducing any possible heat loss that may occur at high temperatures for un-lidded pans [39]. The DSC was routinely calibrated between two points using ultra pure metals, for the lower temperature and heat of fusion indium was used (onset: 156.6°C &  $\Delta H_f$ : 28.45 J/g) and for the upper temperature, zinc (onset: 419.5°C).

In order to remove any previous thermal history introduced into the system during processing the PEEK samples were heated to 400°C and held there for 2 minutes prior to conditioning, fully melting the polymer and giving excellent thermal contact between the sample and pan. This would also act to remove any remaining crystallites which may act as nucleation seeds during subsequent thermal treatments as this is above the thermodynamic melting point ( $T_m$ ) of an infinitely large crystal at 395°C [5].

On conditioning samples it was important to engineer into the polymer a sufficient degree of crystallinity in order to prevent any additional crystallisation on cooling for melt crystallised samples, or on reheating for cold crystallised samples. Therefore when conducting ageing experiments you can be sure that you are investigating the intended morphology and degree of crystallinity engineered into the polymer during sample conditioning, as no additional crystallites would be introduced. For an illustration of the formation of additional crystallinity developed when scanning between  $T_g$  and  $T_m$  refer to Appendix II.

During melt crystallisation in the DSC, samples were rapidly cooled from 400°C to the isothermal crystallisation temperature ( $T_c$ ) at a rate of 160°C/min. This was to ensure that no crystallinity could be introduced prior to reaching the isothermal temperature and that the population of crystals would

be representative solely of those formed at  $T_c$  over the crystallisation time ( $t_c$ ). The semi-crystalline samples were then cooled from  $T_c$  at a constant rate of  $40^\circ\text{C}/\text{min}$  through  $T_g$  to  $80^\circ\text{C}$ , where no further morphological changes are able to take place over a finite time scale. Due to the formation of an adequate degree of crystallinity and using a cooling rate of  $40^\circ\text{C}/\text{min}$  no additional crystallinity formed on cooling between  $T_c$  and  $T_g$ .

In order to cold crystallise samples in the DSC, amorphous PEEK was first obtained by quenching samples from  $400^\circ\text{C}$  directly into liquid nitrogen. The amorphous samples were then rapidly heated from  $80^\circ\text{C}$  to  $T_c$  at  $160^\circ\text{C}/\text{min}$  and isothermally crystallised for  $t_c$ . The samples were then cooled back from  $T_c$  through  $T_g$  to  $80^\circ\text{C}$  at the constant rate of  $40^\circ\text{C}/\text{min}$ . After physical ageing was conducted on the samples due to an adequate degree of crystallinity and a heating rate of  $40^\circ\text{C}/\text{min}$  no further crystallinity was introduced on re-scanning between  $T_g$  and  $T_m$ .

As described earlier, in order to measure the enthalpic relaxation there must be superposability between the aged and un-aged sample traces. Once the desired degree of crystallinity and morphology had been engineered into the samples they were cooled to  $80^\circ\text{C}$  at  $40^\circ\text{C}/\text{min}$ , this is the starting temperature from which samples would be heated to the ageing temperature,  $T_a$ , at  $40^\circ\text{C}/\text{min}$ . The samples were then aged for time,  $t_a$ , and cooled back to  $80^\circ\text{C}$  at  $40^\circ\text{C}/\text{min}$ . The first scan to measure the size of the enthalpy peak developed on ageing was made from  $80^\circ\text{C} - 200^\circ\text{C} - 80^\circ\text{C}$  at  $40^\circ\text{C}/\text{min}$  and the trace stored. Immediately after scanning for the enthalpic peak, the trace for zero ageing time was recorded using the same thermal programme allowing the traces to be subtracted and the enthalpic relaxation to be calculated. So that the precise degree of crystallinity for a specific sample could be calculated the system was scanned to the melt,  $80 - 400^\circ\text{C}$  at  $40^\circ\text{C}/\text{min}$ , allowing the enthalpy of fusion on melting to be measured. As shown in Appendix I, a scanning rate of  $40^\circ\text{C}$  was used as it was found to be in an optimum temperature range that was slow enough to prevent significant thermal lag yet fast enough to prevent large scale reorganisation on heating and cooling.

It is important to note the above discussion provides an overview of the general sample conditioning for melt crystallisation, cold crystallisation, ageing and measurement of enthalpic relaxation. Due to the individual experimental nature of investigations conducted in this work, aspects of the methodology described above have been adapted accordingly. For clarity experimental specific sample conditioning sections are detailed prior to the discussion of results in each of the following sections, 3.1, 3.2, 3.3, 3.4, 3.5.

## Chapter 3 : Results and Discussion

---

### 3.1 Influence of Cooling Rate on Enthalpic Relaxation in Amorphous PEEK

It is known that the rate at which you cool through  $T_g$  has a considerable effect on the resulting ageing kinetics as the point at which the amorphous polymer falls out from a state of equilibrium above the glass transition temperature is determined by the cooling rate imposed on the system [19, 48]. A faster cooling rate gives less time for the molecular chains to accommodate the change in temperature. This causes the system to deviate further from equilibrium at a higher temperature and thus gives the system a greater degree of excess enthalpy to be recovered on ageing as it tends towards equilibrium [48]. The following describes how such an effect was observed in amorphous PEEK.

#### 3.1.1 Sample Conditioning

A series of amorphous PEEK samples were obtained by quenching directly into liquid nitrogen from the melt, and were confirmed to be amorphous (or of equal low crystallinity  $< 2\%$ ) by later scanning on the DSC. They were heated from  $80 - 160^\circ\text{C}$  at a controlled rate of  $40^\circ\text{C}/\text{min}$  and cooled back through  $T_g$  at a specified rate of 5, 10, 20, 40,  $80^\circ\text{C}/\text{min}$ . All samples with specified cooling rates were aged at  $135^\circ\text{C}$  ( $T_a$ ) for 60 mins ( $t_a$ ). They were then heated between  $80 - 160^\circ\text{C}$  at  $40^\circ\text{C}/\text{min}$  and cooled back between  $160 - 80^\circ\text{C}$  at their specified individual cooling rate to obtain the endothermic peak and repeated for a trace of zero ageing time, to obtain the aged and un-aged traces respectively. Heating up to  $160^\circ\text{C}$  was shown to be high enough above  $T_g$  in order to fully relax the amorphous samples yet low enough to prevent the introduction of any crystallinity into the samples as shown on finally scanning the samples into the melt in Figure 3.1.a.

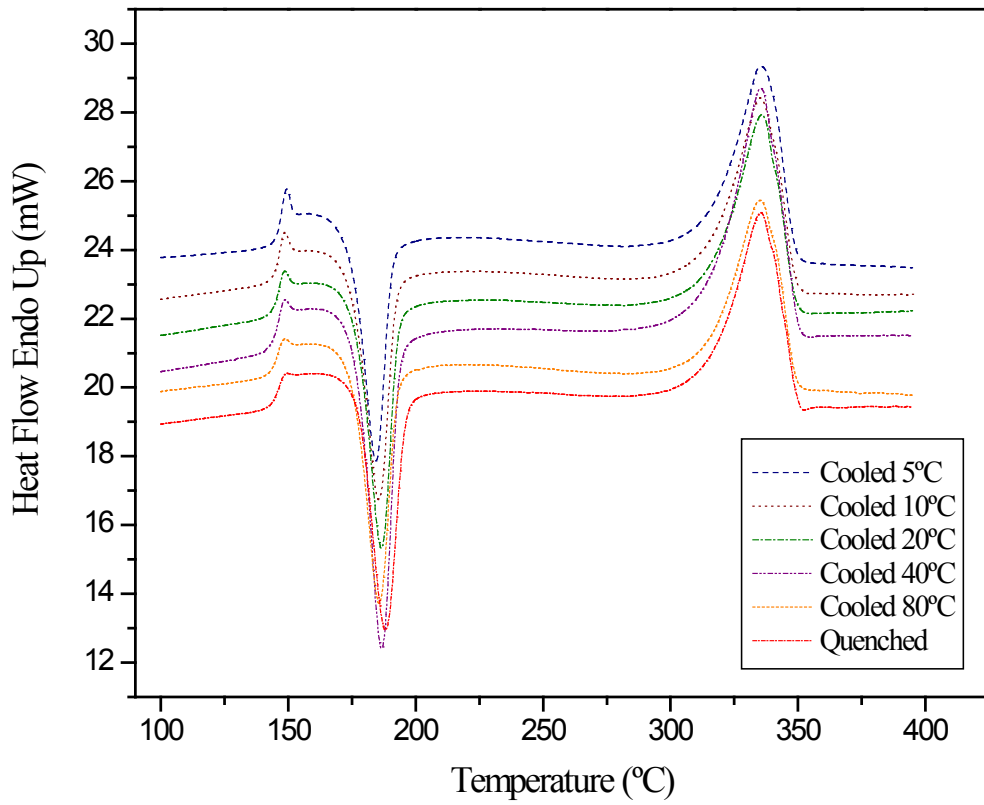


Figure 3.1.a. Melting traces of amorphous samples previously cooled through  $T_g$  at various rates. (Cooling Rate:  $^{\circ}\text{Cmin}^{-1}$ )

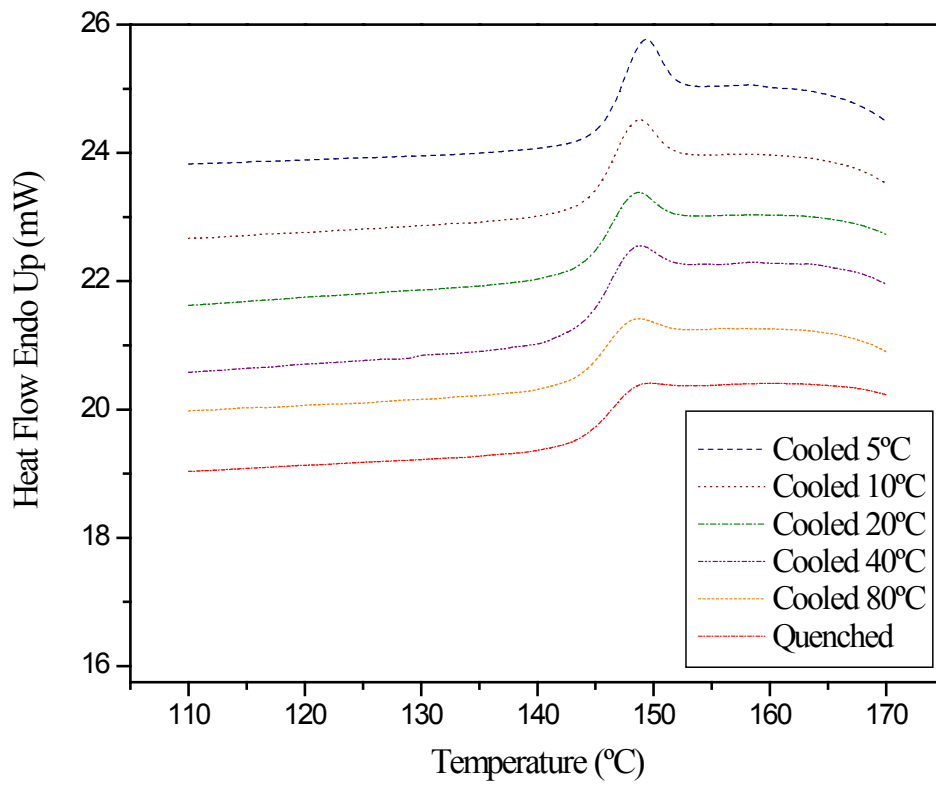


Figure 3.1.b.  $T_g$  region on heating amorphous samples previously cooled through  $T_g$  at various rates. (Cooling Rate:  $^{\circ}\text{Cmin}^{-1}$ )



### 3.1.2 Results and Discussion

The effect of cooling rate on the size of the resulting enthalpic peak recovered on heating through  $T_g$  can be seen clearly in Figure 3.1.b. As described earlier, the slower you cool from the equilibrium liquid state through  $T_g$  into the non-equilibrium glassy state, the more time is available for the molecular chains to accommodate this change in temperature [19, 48], resulting in them ultimately having to relax less in order to reach  $H_\infty$ . However, it appears in Figure 3.1.b that there is a greater enthalpic peak developing on  $T_g$  with slower cooling rates. This can be assigned to the fact that the slower the sample is cooled, a longer time period is spent at temperatures in close proximity to the  $T_g$  where rates of relaxation are highest. In effect the slow cooled samples are already being aged on cooling when compared to the fast cooled samples which spend comparatively little time in the small temperature range below  $T_g$  where physical ageing can take place [48].

However when subtracting the trace for zero ageing time from that of the aged trace for the same sample, as they have both been cooled through  $T_g$  at an identical rate any ageing introduced on cooling through  $T_g$  is negated. It is for this reason the two traces must superimpose perfectly so only the enthalpic relaxation introduced on ageing is measured.

As shown in Figure 3.2 for a given ageing time much more relaxation is seen on ageing the fast cooled samples as they are further from equilibrium and also have undergone less relaxation on cooling. It is clear that during slow cooling the samples did not reach thermodynamic equilibrium as further relaxation is seen on ageing. However because some relaxation has already occurred on cooling as they continue to approach  $H_\infty$  relaxation times increase, so less enthalpic relaxation is developed on ageing for the same  $T_a$  and  $t_a$  when compared to the fast cooled samples [48].

It is therefore important to control the cooling rate through  $T_g$  as this has been shown to affect the subsequent degree of enthalpic relaxation on ageing [19]. This can be achieved by cooling at a constant  $40^\circ\text{C}/\text{min}$  from a state of equilibrium for all samples prior to ageing experiments.

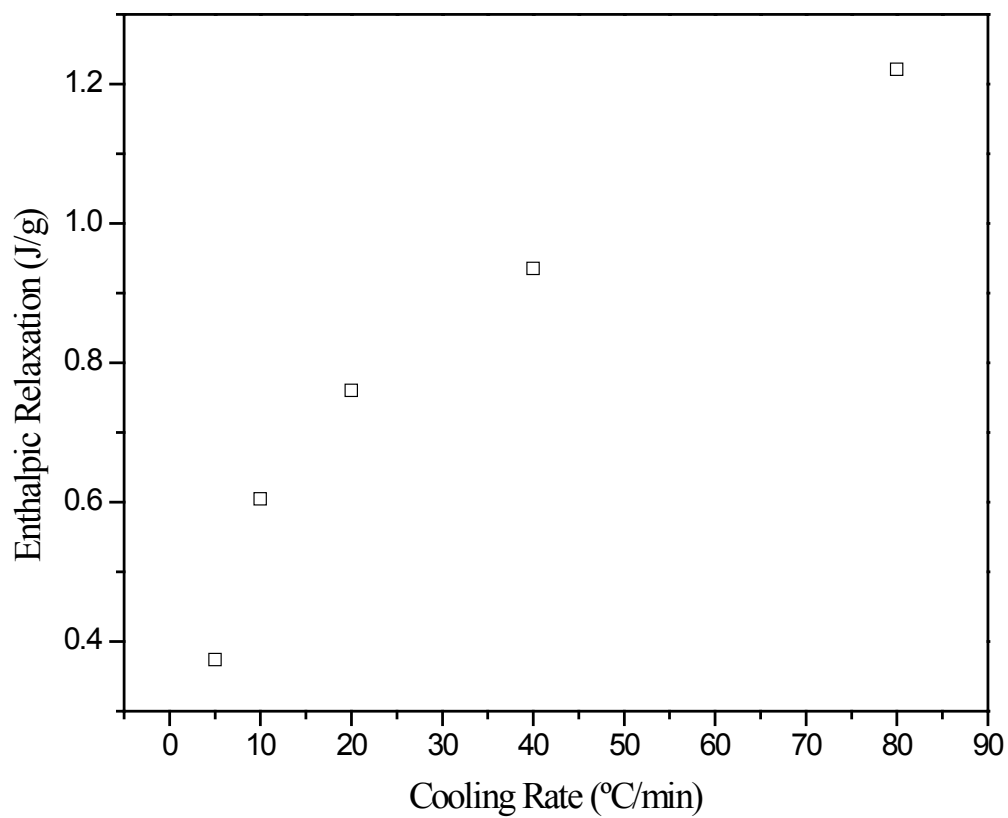


Figure 3.2. Enthalpic relaxation as a function of cooling rate for amorphous samples cooled through  $T_g$  at various rates and aged at  $135^\circ\text{C}$  for 60 mins.

### **3.2 Influence of Crystallinity on Enthalpic Relaxation**

As discussed above the rate at which amorphous samples are cooled through the glass transition region influences the overall degree of enthalpic relaxation, thereby controlling the cooling rate through  $T_g$  this effect can be controlled for. Despite cooling rate having a significant influence on the ageing kinetics of amorphous polymer, the introduction of crystallinity into a sample has been shown to reduce the overall degree of enthalpic relaxation due to a reduction of amorphous fraction and a restriction of chain mobility in the amorphous regions by crystallites [31, 49]. Therefore although cooling rate is standardised it is not thought that such a profound effect will be seen for semi-crystalline PEEK, which shall now be further investigated in this work.

#### **3.2.1 Sample Conditioning**

As a semi-crystalline polymer PEEK can be crystallised in a number of ways, as previously introduced. In order to obtain samples of varying degrees of crystallinity one set of samples were non-isothermally crystallised from the melt to room temperature at 10, 20, 40 and 60°C/min. They were then rescanned up to 200°C and back to 80°C at 40°C/min to engineer a controlled cooling rate through  $T_g$  into the samples.

A second set of samples was conditioned by isothermally crystallising samples at 300, 305, 310 and 315°C for 5, 10, 15 and 30 minutes respectively to give a controlled degree of crystallinity but varying morphology, before cooling from  $T_c$  to below  $T_g$  at 40°C/min.

All samples were aged at 142°C for 180 and 3600 minutes before the enthalpic recovery and zero-ageing traces were obtained and subtracted as outlined in the experimental. Sample crystallinity was subsequently measured on scanning samples into the melt and measuring the heat of fusion.

### 3.2.2 Results and Discussion

For non-isothermally crystallised samples on cooling from the melt at various rates it can be seen in Figure 3.3.a that slower cooling rates allow the onset of crystallisation to occur at higher temperatures as there is more time for nucleation and growth of crystallites [15]. In addition to this isothermally crystallised samples held at lower temperatures are able to crystallise at much higher rates due to more favourable nucleation and growth conditions as shown by the increase in size of the exothermic peak in Figure 3.3.b. Once the desired morphology had been engineered into the samples they were aged at the same  $T_a$  for an equal  $t_a$ .

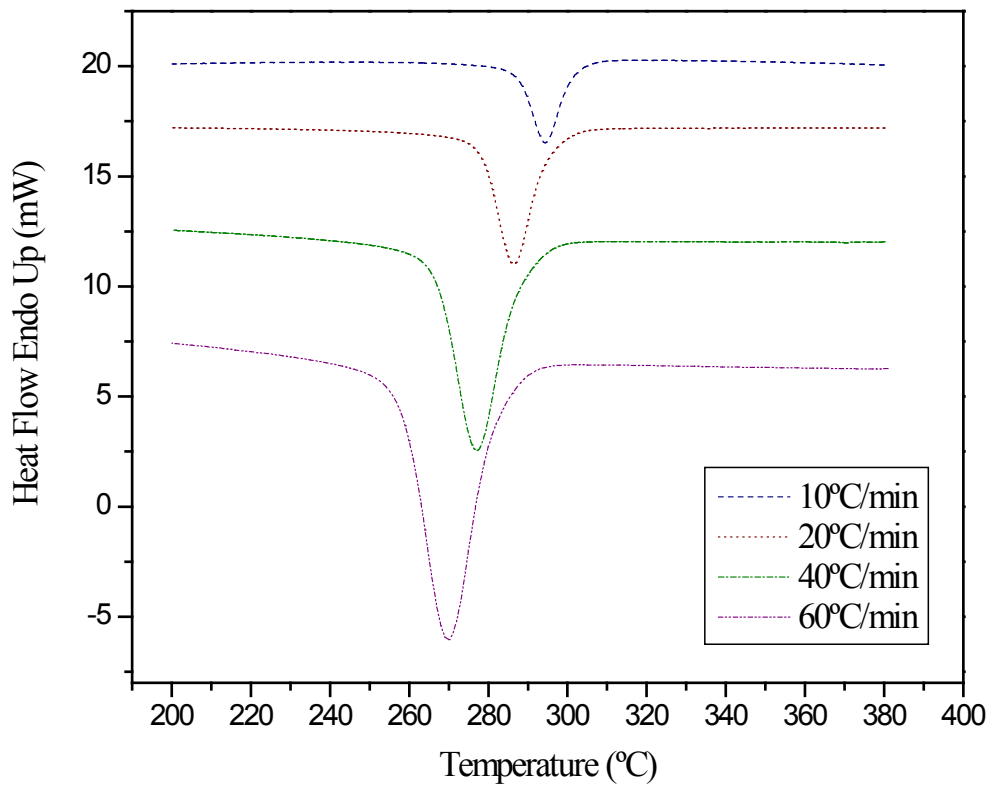


Figure 3.3.a. Non-isothermal crystallisation traces for samples cooled from the melt at various rates.

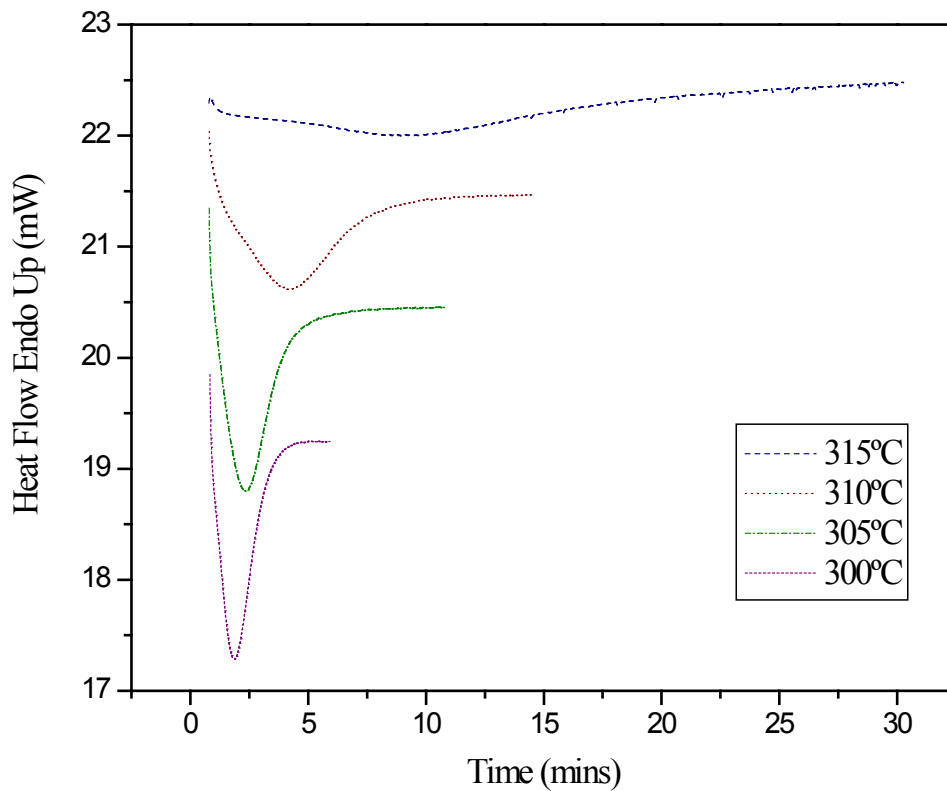


Figure 3.3.b. Isothermal crystallisation traces of samples held at a given  $T_c$  for various lengths of time.

Due to variations in enthalpic relaxation between non-isothermal and isothermally crystallised samples and also variations between inter-sample data sets, for clarity only the samples with the upper and lower degrees of crystallinity are displayed in Figure 3.4. Samples slow cooled from the melt at 10 and 20°C/min obtained a degree of crystallinity of  $36 \pm 0.5\%$  and  $35 \pm 0.5\%$  respectively, whereas those isothermally crystallised at 300 and 315°C were controlled to  $30.50 \pm 0.5\%$  crystallinity.

As expected with an increase in the degree of crystallinity the enthalpic relaxation observed at a given ageing temperature and time is shown to decrease [31, 32, 34]. Figure 3.4 demonstrates that for an equal  $T_a$  and  $t_a$  the isothermally crystallised samples of a lower crystalline content are able to relax to a greater extent than the non-isothermally crystallised samples with a higher degree of crystallinity.

This could easily be assigned to the reduction of amorphous fraction present in the isothermally crystallised samples, however as it was difficult to establish significant trends across these data sets it is likely that the system is not so simple. Despite controlling the degree of crystallinity for isothermally crystallised samples, although they showed more ageing than samples of a higher crystalline fraction, the inter-data sets were considerably scattered. This makes a meaningful interpretation of the effect of lamellae size on relaxation more difficult, and suggests the crystal/amorphous interface has a considerable influence on ageing characteristics [31].

Therefore the focus of this work now turns to investigating how the glass transition is influenced by crystallinity, and more importantly crystalline morphology, so that a specific ageing temperature can be tailored to an individual polymer system. As isothermal crystallisation allows a greater degree of control over the size and number of crystallites developed, by altering  $T_c$  and  $t_c$ , this method is adopted in order to engineer a desired morphology into the sample.

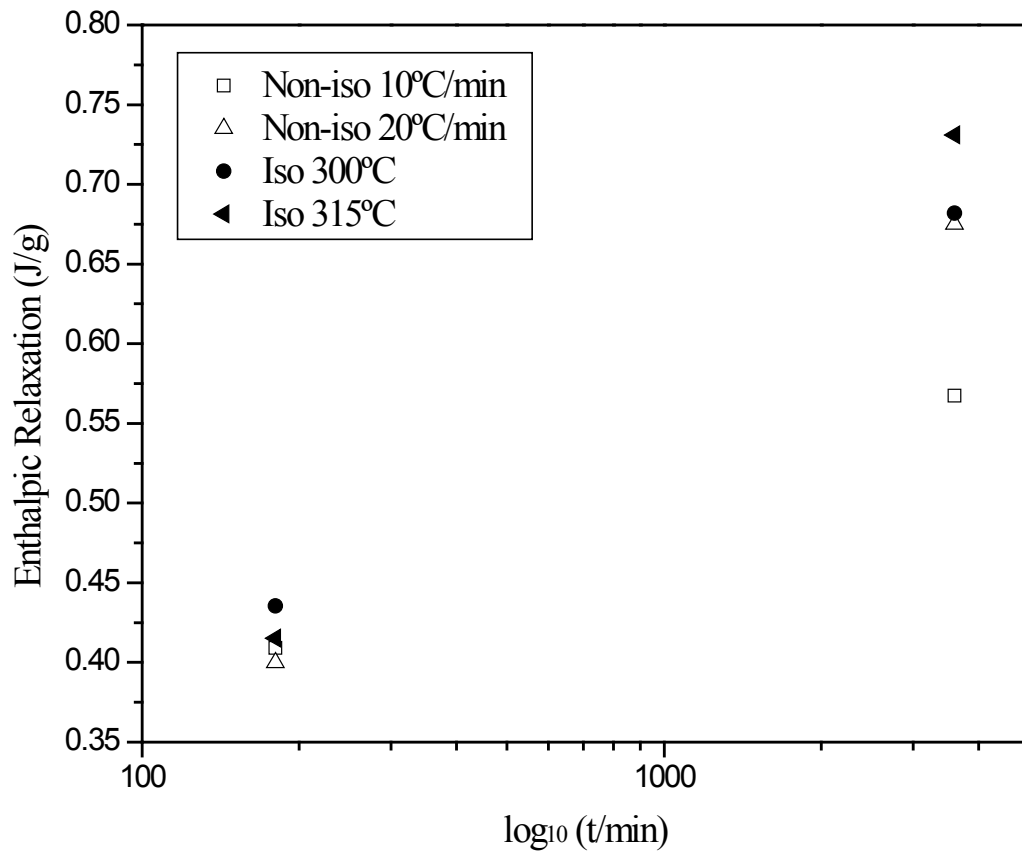


Figure 3.4. Enthalpic relaxation as a function of log time for isothermally and non-isothermally crystallised samples with varying degrees of crystallinity. Non-isothermally crystallised at 10 and 20°C/min : 36 and 35 ± 0.5% crystalline respectively. Isothermally crystallised at 300°C 5 mins and 315°C 30 mins: 30 ± 0.5% crystalline each.

### **3.3 Effect of Crystallinity on the Glass Transition**

In Section 3.2 an increase in crystallinity has been shown to reduce the overall degree of enthalpic relaxation. However it was difficult to establish any significant inter-data trends suggesting that the selection of an ageing temperature should be considered more carefully with regards to sample crystallinity and morphology. As the presence of crystallites has previously been shown to affect the glass transition temperature by reducing segmental mobility of the amorphous phase [24, 25], it shall now be further investigated in this work with regards to PEEK.

#### **3.3.1 Sample Conditioning**

In order to obtain samples of the same morphology with crystallites grown under identical isothermal conditions, but with varying degrees of crystallinity, PEEK samples were quenched from the same crystallisation temperature directly into liquid nitrogen after varying lengths of time. The crystallisation temperature used was 312°C with the following isothermal times 0, 2, 4, 6, 10, 20, 30, 60 minutes. Samples were then scanned from 80 – 400°C at 40°C/min in order to measure T<sub>g</sub> and calculate degree of crystallinity. The crystallinity developed at the isothermal crystallisation temperature over the varying crystallisation times was determined by subtracting the exothermic crystallisation peak from the endothermic melting peak [Appendix II].

It is important to note that no further conditioning scans were performed on the samples prior to the melting scan. This is due to the varying degrees of crystallinity present in the samples which would cause greater amounts of relaxation in the amorphous samples on cooling through T<sub>g</sub>, thus making the accurate determination of T<sub>g</sub> much more difficult. Although an exact cooling rate has not been engineered into the samples, the rate at which they have been quenched through T<sub>g</sub> has at least been considered and controlled for as they were all processed and quenched through T<sub>g</sub> under identical conditions.



### 3.3.2 Results and Discussion

It can be seen in Figure 3.5 that as an increasing degree of crystallinity is developed over a longer crystallisation time, the breadth of the glass transition is gradually increased. This is due to the effect of crystallinity reducing the mobility of the amorphous phase, with the amorphous chains in closer proximity to the crystal surface experiencing a greater degree of restriction [24, 25, 33]. Therefore with an increasing degree of crystallinity more chains are constrained to a greater degree at the crystal/ amorphous interface and require higher temperatures in order to mobilise, resulting in the increased breadth of the transition.

The effect of increasing crystallinity is also shown to push the measured thermodynamic glass transition upwards as shown in Figure 3.6, again due to the higher temperatures required in order for more constrained amorphous regions to mobilise. It is important to note that the samples were isothermally crystallised at the same temperature and under the same conditions before they were quenched after an individual  $t_c$ . Therefore the crystallisation kinetics for nucleation and growth of the crystallites is the same across the samples resulting in a standard morphology of the lamellae crystals. It is only the degree of crystallinity developed that has been altered between samples and which has subsequently influenced the glass transition.

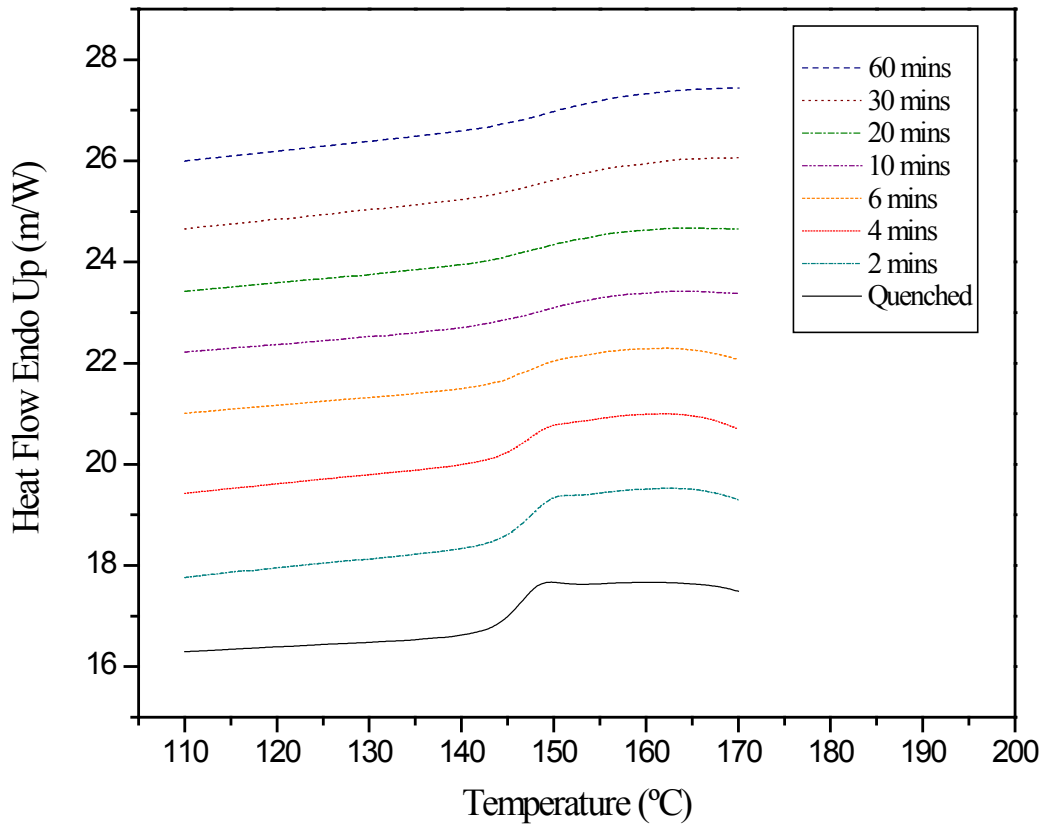


Figure 3.5. Broadening of the glass transition with increasing crystallinity developed on longer isothermal holding times at a 312°C.

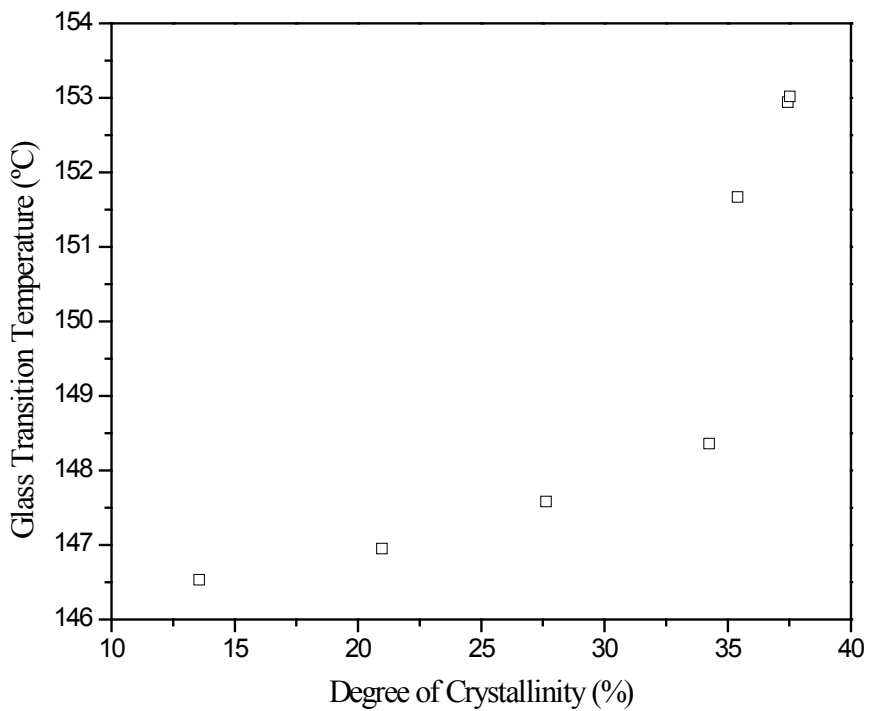


Figure 3.6. Glass transition temperature as a function of crystallinity. The measured thermodynamic position of T<sub>g</sub> is pushed to increasingly higher temperatures with the development of crystallinity.

### **3.4 Effect of Isothermal Crystallisation Temperature on the Glass Transition**

As discussed above for samples isothermally crystallised at the same temperature for various times the degree of crystallinity can have a significant effect on the breadth and measured position of the glass transition temperature. Therefore in order to investigate the influence of crystalline morphology on  $T_g$ , as determined by the isothermal crystallisation temperature, degree of crystallinity must be kept constant across melt crystallised and cold crystallised samples.

#### **3.4.1 Sample Conditioning**

Figure 3.7.a and Figure 3.7.b show PEEK samples being cooled from the melt and heated from the quenched amorphous state at 160°C/min respectively in order to determine a suitable  $T_c$  to use before the onset of crystallisation. Melt crystallised samples were cooled from the melt to  $T_c$  at 160°C/min and isothermally held for  $t_c$  before cooling at 40°C/min to room temperature, no further crystallisation was seen on cooling. Quenched amorphous samples were heated from 80°C to  $T_c$  at 160°C/min and again isothermally held for  $t_c$  before cooling back down at 40°C/min to room temperature. All samples were then scanned to the melt at 40°C/min and the traces recorded in order to determine the glass transition temperature and heat of fusion on melting. Individual isothermal crystallisation temperatures and corresponding times used in order to allow a similar degree of crystallinity ( $31 \pm 1\%$ ) to develop are detailed in Table 3.1.

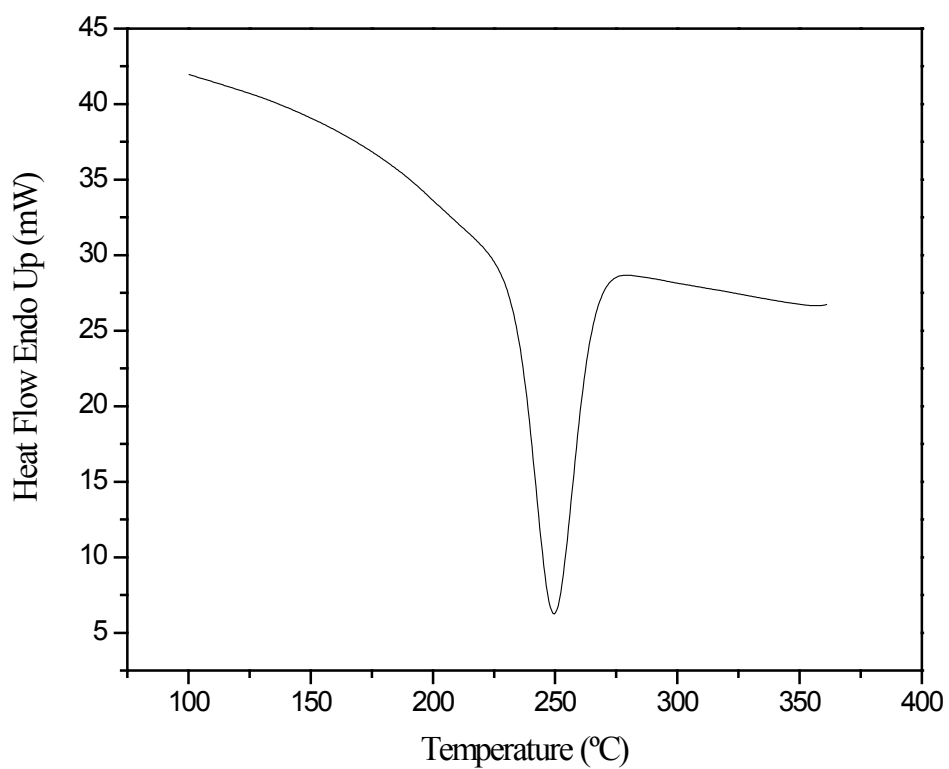


Figure 3.7.a. Trace recorded on cooling from the melt to below  $T_g$  at  $160^\circ\text{C}/\text{min}$ . For use in determining appropriate isothermal temperatures for melt crystallisation.

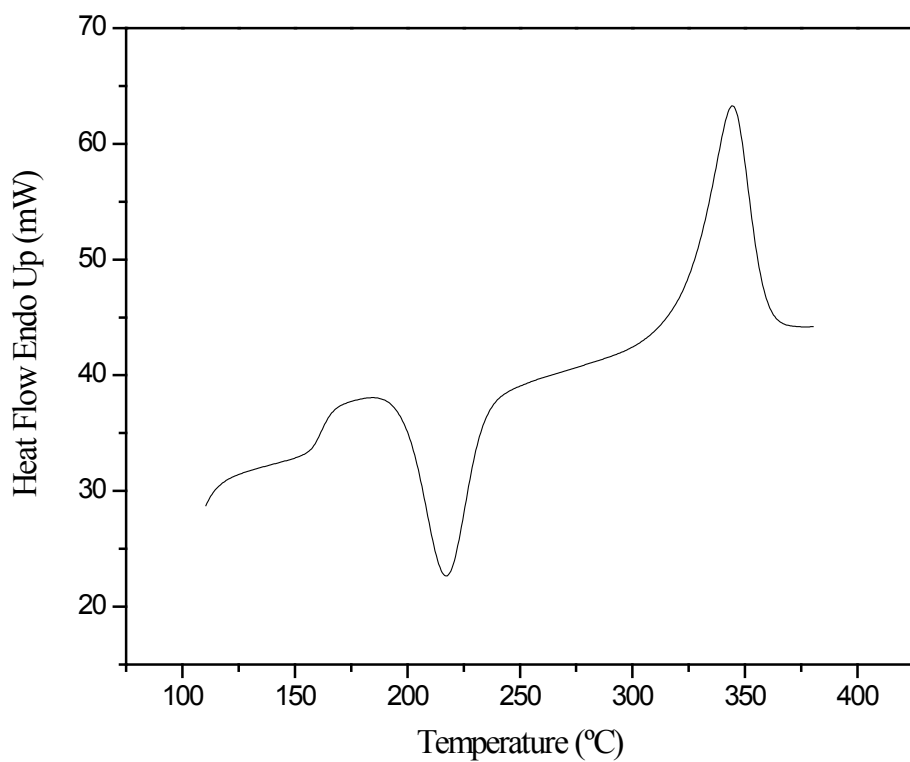


Figure 3.7.b. Trace recorded on scanning a quenched amorphous sample from below  $T_g$  into the melt at  $160^\circ\text{C}/\text{min}$ . For use in determining appropriate isothermal temperatures for cold crystallisation.

Table 3.1. Isothermal crystallisation temperatures, times and corresponding glass transition temperature along with degree of crystallinities for cold and melt crystallised samples.

Cold Crystallised Samples				Melt Crystallised Samples			
Tc (°C)	tc (min)	Tg (°C)	Xc (%)	Tc (°C)	tc (min)	Tg (°C)	Xc (%)
200.0	10	159.5	31.03	250.0	3	155.6	31.27
202.0	10	159.0	30.98	260.0	3	155.2	31.88
210.0	5	158.8	31.42	270.0	3	154.3	31.57
215.0	3	158.8	31.60	280.0	3	154.1	31.62
				290.0	5	153.2	31.60
				300.0	7	152.9	31.34
				305.0	10	152.5	31.03
				310.0	15	152.5	30.25
				315.0	30	152.3	30.25
				320.0	60	152.1	30.18

### 3.4.2 Results and Discussion

In order to obtain a population of crystals which are perfectly representative of a particular isothermal crystallisation temperature it is important that nucleation has not begun prior to the sample reaching  $T_c$ . However in practice this was very difficult to achieve, especially for cold crystallised samples, despite the fast heating rate used. As shown in Figure 3.7.b there is a very limited temperature range above the  $T_g$  and below the onset of crystallisation where a single population of crystals can be developed. In addition to this further complications arise if you attempt to crystallise at temperatures just above  $T_g$ . The development of the lower endotherm at temperatures slightly above  $T_c$  makes it very difficult to extrapolate the liquid line needed to measure  $T_g$ , as the onset of crystal melting has already begun before equilibrium is established. Therefore a number of cold crystallised and melt crystallised samples had to be held at isothermal temperatures where the onset of crystallisation had already begun.

However it is important to note that even for melt crystallised samples isothermally held above  $290^\circ\text{C}$  where all the crystals are formed at  $T_c$  there is still a broad melting endotherm showing that a range of crystallite sizes are present within the sample, a factor inherent to polymer morphology [12].

Although in some samples nucleation may have begun prior to reaching the isothermal temperature, due to the time spent at  $T_c$  a sufficient degree of crystallinity is introduced for the measured  $T_g$  to be taken as representative of a crystal population formed at that temperature. This is supported by the development of an endotherm slightly above  $T_c$  which is indicative of crystal growth at a given isothermal temperature, as shown in Figure 3.8 and previously discussed with regards to multiple melting endotherms. When calculating the degree of crystallinity for the samples, the heat of fusion for the small endotherm developed during secondary crystallisation at  $T_c$  was added to that of the upper melting peak of the larger, primary crystals. It is not thought that the smaller endotherm can be representative of the whole degree of crystallinity formed at  $T_c$  as suggested by the melting and recrystallisation theory as it is too small. However, it is not disputed that on scanning some melting and recrystallisation of the crystals may be seen at slow scanning rates [Appendix I].

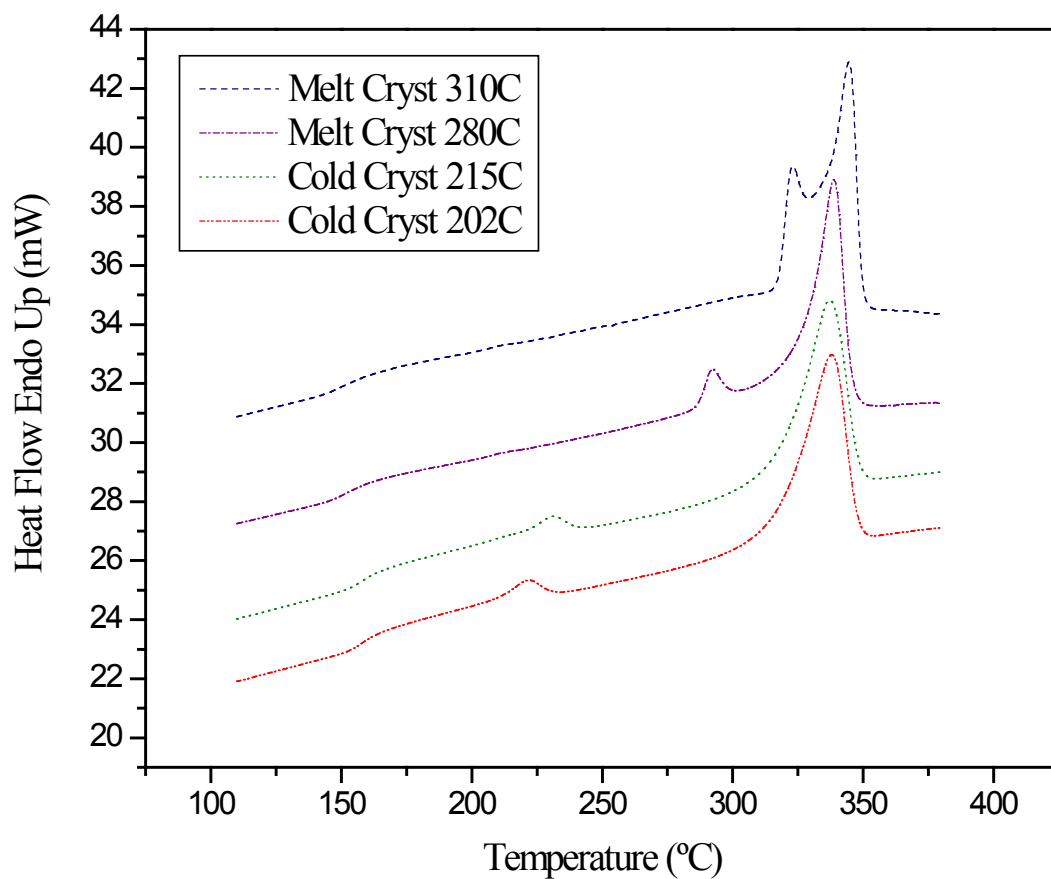


Figure 3.8. A selection of traces for cold and melt crystallised samples scanned from below  $T_g$  into the melt. Note the development of a smaller endothermic peak at temperatures slightly above the individual  $T_c$ .

From Figure 3.9 it can be seen that for a controlled degree of crystallinity the isothermal crystallisation temperature has a strong influence on the glass transition. Samples crystallised from the melt at higher temperatures have increasingly larger, but fewer crystallites which corresponds to a decrease in the glass transition temperature. As all samples have an equal degree of crystallinity, and therefore an equal amorphous fraction, it follows that the larger crystallites are made up of fewer but thicker lamellae [31, 49]. Due to the reduced number of lamellae there is a smaller surface area at the crystal/amorphous interface. As there is less constraint of the amorphous fraction at the crystal interface there is a greater free amorphous region which is able to mobilise at lower temperatures, resulting in the lower glass transition temperature.

With decreasing  $T_c$  there is an increasing number of progressively smaller and thinner crystallites, giving a greater area at the crystal/amorphous interface which leads to a greater degree of constrained amorphous region and raises the  $T_g$ . The cold crystallised samples are formed in a viscous environment of low molecular mobility making nucleation of crystallites easy but growth much more difficult, giving rise to a population of many much smaller crystals. Again as the crystalline and amorphous content is equal across the samples, the smaller crystallites will have a greater number of thinner lamellae stacks and therefore a much greater crystal/amorphous interface [31, 49]. This greater restricted amorphous fraction requires a higher temperature in order to mobilise and transform from the glassy to liquid state giving the higher glass transition temperature. A modest decrease in  $T_g$  with increasing cold crystallisation temperature has also been shown before in PEEK samples, again assigned to a decrease in the constraint of amorphous chain segments by the crystallites [50].



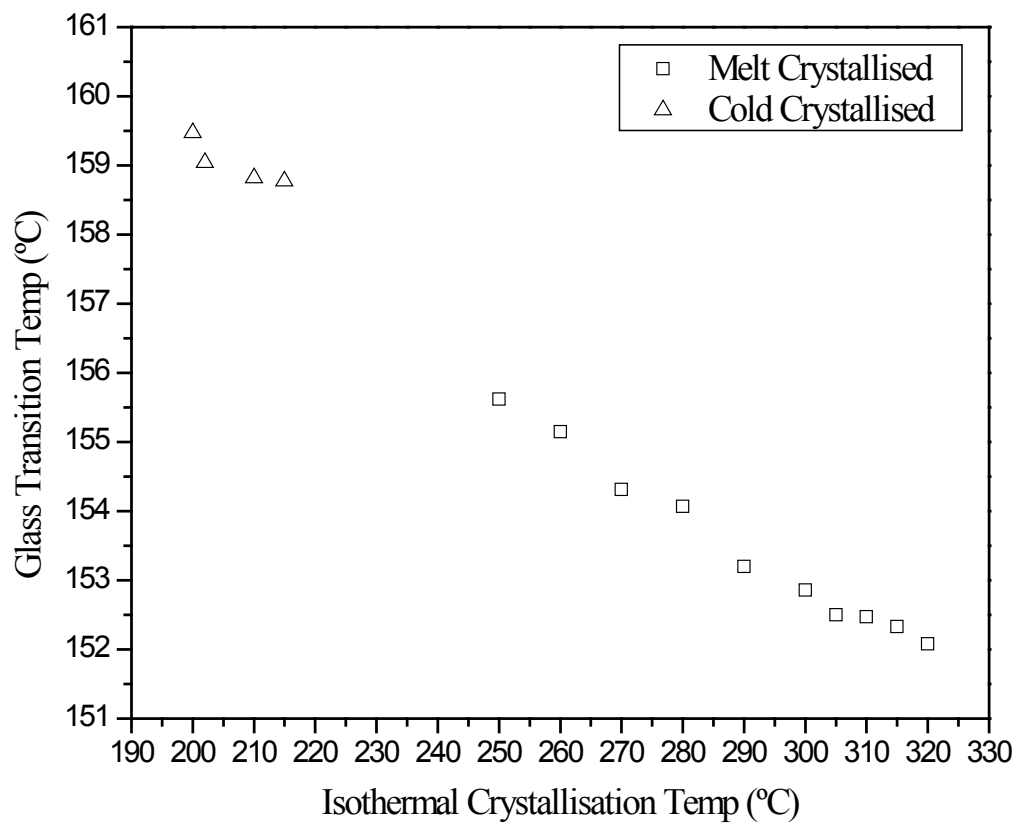


Figure 3.9. The glass transition temperature as a function of isothermal crystallisation temperature for cold and melt crystallised samples.

### **3.5 Effect of Lamellae Thickness on Enthalpic Relaxation**

Due to the effects of crystallinity and crystalline morphology on the glass transition temperature as discussed in the preceding sections, when determining the temperature at which to age samples it is essential to take such factors into account. Even if the degree of crystallinity is controlled the variation in  $T_g$  with lamellae thickness must still be considered. If a standard temperature was set for all ageing experiments this would result in an undercooling considerably closer to the  $T_g$  of some samples than others. As physical ageing and enthalpic relaxation are highly dependent upon the temperature and time the polymer is stored below  $T_g$  such a variation in proximity could produce misleading results [19]. If for example a standard ageing temperature of 145°C was used this would be ~7°C below the  $T_g$  of the upper melt crystallised samples but ~14°C below that of the cold crystallised samples [Figure 3.9]. Therefore accelerated relaxation would be observed for the melt crystallised samples as they would be driven towards equilibrium at faster rates when aged at temperatures approaching the  $T_g$ , compared to little relaxation over the same  $t_a$  in the cold crystallised samples where the ageing temperature is much further from the  $T_g$ .

#### **3.5.1 Sample Conditioning**

The cold and melt crystallised samples were prepared in very much the same way as described in Section 3.4.1 where they were heated or cooled to  $T_c$  and held for  $t_c$  before cooling to room temperature at 40°C/min. In order to control the sample crystallinity to  $31 \pm 1\%$  the cold crystallised samples were held at 202°C and 215°C for 10 and 3 minutes, while the samples isothermally crystallised from the melt were held at 280°C and 310°C for 3 and 20 minutes respectively.

Samples were then aged at an undercooling of 10°C from their individually measured  $T_g$ 's for 180, 360, 900 and 4320 minutes before the trace of  $T_g$  with the endothermic recovery peak and that for zero-ageing time were recorded and subtracted (example Fig. 3.10). In order to confirm the correct degree of crystallinity had been engineered into each of the samples at their respective isothermal

crystallisation temperatures, they were scanned into the melt and the heat of fusion on melting from the double endothermic peaks was recorded. The measured degree of crystallinity, along with  $T_g$  and ageing temperature for cold crystallised and melt crystallised samples are detailed in Table 3.2.a and 3.2.b respectively.

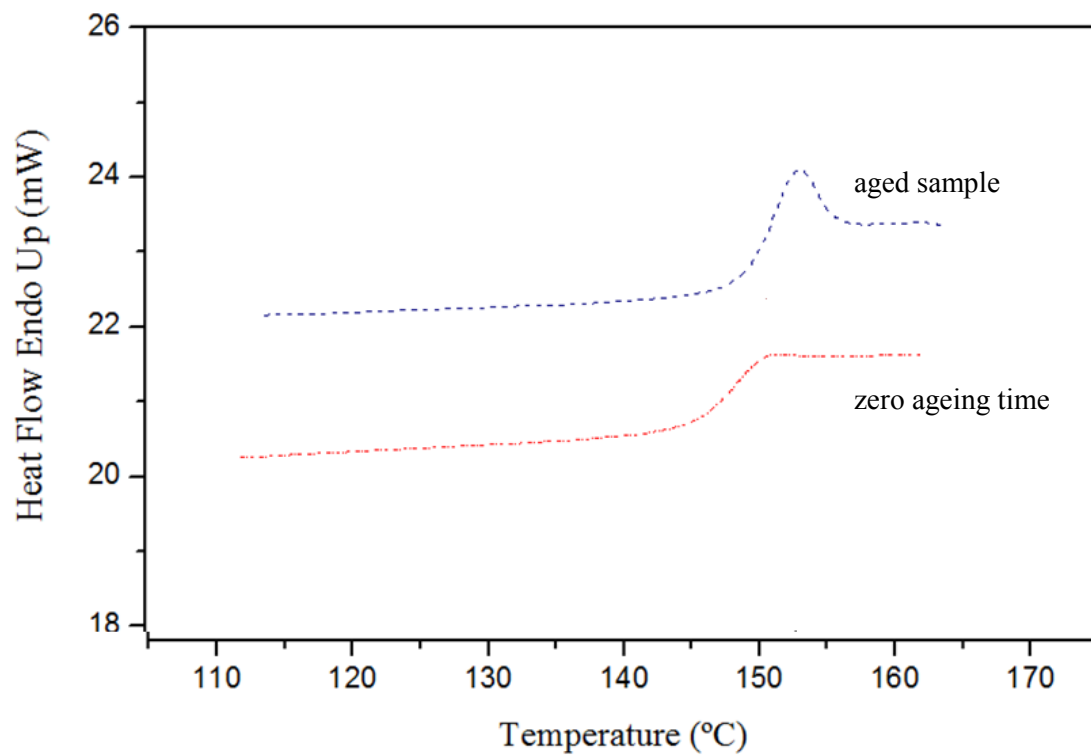


Fig 3.10. To calculate degree of enthalpic relaxation, the trace for zero ageing time was subtracted from that of an aged sample.

Table 3.2.a. The individual glass transition temperatures (T<sub>g</sub>), ageing temperatures (T<sub>a</sub>) and degree of crystallinity (X<sub>c</sub>) for different ageing times (t<sub>a</sub>) of cold crystallised samples.

<b>Cold Crystallised</b>						
	202°C 10 mins			215°C 3 mins		
t <sub>a</sub> (mins)	T <sub>g</sub> (°C)	T <sub>a</sub> (°C)	X <sub>c</sub> (%)	T <sub>g</sub> (°C)	T <sub>a</sub> (°C)	X <sub>c</sub> (%)
180	158.8	149.0	30.87	158.5	148.5	30.52
360	159.1	149.0	31.01	158.7	148.5	30.59
900	159.2	149.0	30.74	158.5	148.5	31.36
4320	159.2	149.0	31.25	159.2	149.0	31.05

Table 3.2.b. The individual glass transition temperatures (T<sub>g</sub>), ageing temperatures (T<sub>a</sub>) and degree of crystallinity (X<sub>c</sub>) for different ageing times (t<sub>a</sub>) of melt crystallised samples.

<b>Melt Crystallised</b>						
	280°C 3 mins			310°C 20 mins		
t <sub>a</sub> (mins)	T <sub>g</sub> (°C)	T <sub>a</sub> (°C)	X <sub>c</sub> (%)	T <sub>g</sub> (°C)	T <sub>a</sub> (°C)	X <sub>c</sub> (%)
180	153.5	143.5	30.98	152.4	142.5	31.55
360	154.2	144.0	31.81	152.4	142.5	31.55
900	153.3	143.5	31.54	152.9	143.0	31.59
4320	154.1	144.0	31.82	153.0	143.0	31.57

### 3.5.2 Results and Discussion

In compensating for the shift in  $T_g$  with crystalline morphology and eliminating the influence of degree of crystallinity on glass transition, it has been possible to directly investigate the effect of lamellae thickness on physical ageing kinetics. The degree of enthalpic relaxation for 2 cold crystallised and 2 melt crystallised samples, aged for varying lengths of time is shown in Figure 3.11.

In this work it has been shown that an increase in the degree of crystallinity along with a reduction in the size of crystallites acts to raise the glass transition temperature of the polymer. This has been credited to an increase in the area of the crystal/amorphous interfacial region giving a greater degree of constrained amorphous fraction, which requires higher temperatures in order to mobilise. By taking this into account and ageing at an equal undercooling of  $10^\circ\text{C}$  tailored to the  $T_g$  of the system, Figure 3.11 shows that cold crystallised samples undergo a greater degree of enthalpic relaxation for the same degree of crystallinity over a given ageing time.

This may seem counterintuitive as the increased constrained amorphous fraction introduced by the numerous, small lamellae has previously been shown to increase  $T_g$  due to a greater restriction of amorphous material at the crystal/amorphous interface. However, a similar finding has been reported in poly(phenylene sulfide) where the semi-crystalline polymer is again described using a three-phase model [51]. It is proposed that an increased constrained amorphous phase actually helps to accelerate the ageing kinetics when compared to the free amorphous phase. This is because the constrained phase would consist of a greater number of tightly packed chain segments so can increase the rates of relaxation as more segmental molecular relaxations would be able to contribute to the process [51, 52]. Even though the mobility of this tightly packed restricted amorphous phase may be lower, there are more segments involved in the relaxation process than in the free amorphous phase, so are able to contribute more effectively and ultimately accelerate the ageing process [52, 53].

Interestingly in semi-crystalline PEEK the constraint of the amorphous phase by crystallites has previously been shown to increase the co-operativity of the relaxation process [32] and samples with larger amounts of constrained amorphous fraction have been shown to relax more [54].

Despite the possibility of the increased constrained amorphous fraction in cold crystallised samples causing the acceleration of enthalpic relaxation, it is important to remember that due to a higher  $T_g$  they were also aged at a higher temperature. Therefore although there may be less free amorphous material in the cold crystallised samples (as there is a greater degree of the constrained phase) this would be aged at a higher temperature than the free amorphous phase of the melt crystallised samples and may be the cause of the greater degrees of ageing seen.

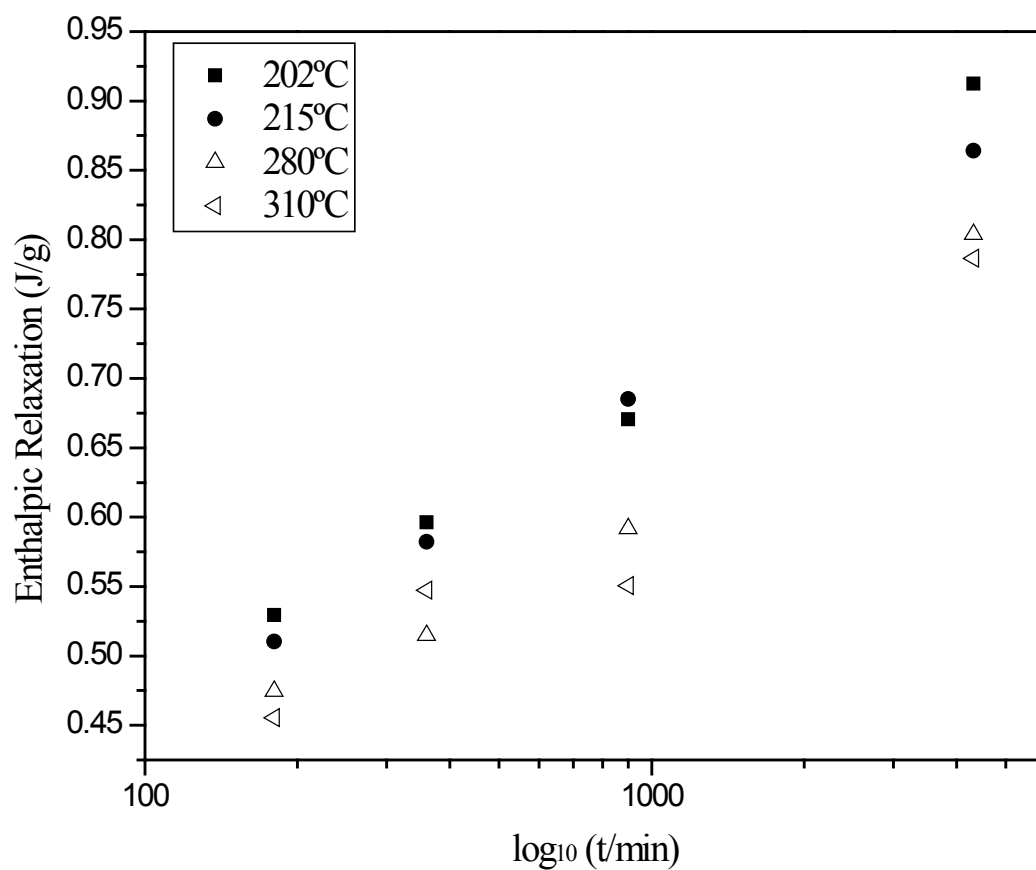


Figure 3.11. The degree of enthalpic relaxation against log time of cold crystallised and melt crystallised samples of an equal degree of crystallinity aged at an undercooling of 10°C below individual Tg's.



It then becomes important to investigate the measured onset, end and breadth of the glass transition in order to determine whether or not this can account for the increased relaxation observed. Average values of samples isothermally crystallised at the specified temperatures and over the 4 ageing times are given in Table 3.3.

In this work the glass transition temperature was taken to be the mid-point of the sigmoidal trace where lines from the glass and liquid phase could be extrapolated to meet [45, 46, 47] with the ageing temperature set at an undercooling of 10°C from this ‘thermodynamic’ T<sub>g</sub>. However as shown in Table 3.3 the onset of the glass transition for the melt crystallised samples is at a lower temperature and the transition itself is much broader than that of the cold crystallised samples. Due to this increased breadth the average onset for the upper melt crystallised sample [T<sub>c</sub> 310°C] is found to be ~10°C below its thermodynamic T<sub>g</sub>. As the ageing temperature was set at 10°C below the thermodynamic T<sub>g</sub> measurement, it has been aged very close to the onset of the glass transition when compared to that of the cold crystallised sample [T<sub>c</sub> 202°C] whose onset is ~7°C below its thermodynamic T<sub>g</sub>. Therefore you may expect a greater degree of enthalpic relaxation to be seen in the melt crystallised samples, from unconstrained amorphous regions which are able to mobilise at temperatures close to the T<sub>g</sub> onset [19]. Although this may contribute initially (giving relaxation values closer to those seen in cold crystallised samples over shorter ageing times), despite the cold crystallised samples being aged further from their T<sub>g</sub> onset, for the same ΔT of 10°C they continually exhibit a greater degree of enthalpic relaxation. This supports the hypothesis that the additional constrained amorphous phase in the cold crystallised samples is able to accelerate the ageing process due to a greater degree of molecular packing.

Again due to the breadth of the transition, when looking at the T<sub>g</sub> end, the value for the cold crystallised sample [T<sub>c</sub> 202°C] is only ~4°C above that of the melt crystallised sample [T<sub>c</sub> 310°C] as opposed to being ~10°C greater in the onset measurements. It is clear that the much more compact and higher T<sub>g</sub> values of the cold crystallised samples are due to the increased constraint of the amorphous phase at the crystal/amorphous interface of the thinner and more numerous lamellae.

Table 3.3. Average values of Tg measurements for isothermally crystallised samples.

Iso Temp (°C)	Thermodynamic Tg (°C)	Tg Onset (°C)	Tg End (°C)	Tg Breadth (°C)	Average Ageing Temp (°C)	Xc (%)
202.0	159.1	152.6	164.7	12.1	149.0	30.97
215.0	158.7	152.4	164.8	12.4	148.6	30.88
280.0	153.8	144.9	161.4	16.5	143.8	31.54
310.0	152.7	142.8	160.1	17.3	142.8	31.57

For the same degree of crystallinity there is less crystal/amorphous interface for melt crystallised samples with thicker lamellae which, although still act to constrain the amorphous region adjacent to the crystal face, allow mobilisation of the constrained phase at a lower temperature. As there is less constraint on polymer chains furthest from the crystal interface these are able to relax soon after the free amorphous phase [24]. Those in close proximity to crystals are far more entangled, so extend the  $T_g$  breadth. However as the  $T_g$  end is still below that for cold crystallised samples it suggests that molecular motion at the interface is less restricted.

The increased restriction of the amorphous phase in cold crystallised samples can be attributed to the development of crystallites in an increasingly restricted environment. As described by the nucleation theory the mobility of polymer chains is closely related to temperature [12, 15]. At low temperatures there is less molecular mobility, creating a highly entangled and viscous system. As there is less mobility in the system growth of ordered structures becomes more difficult, so during crystallisation polymer chains which are unable to crystallise may become increasingly entangled and tethered across lamellae giving rise to a greater degree of constrained amorphous fraction [29, 30]. On crystallising at higher temperatures the chains have a greater deal of molecular mobility so once nucleation has begun they are able to transport to the ends of growing lamellae stacks and contribute to the growing crystal interface with a lesser degree of entanglement.

It is this increased constraint of the amorphous phase in cold crystallised samples and its higher degree of packing during crystallisation which on ageing allows the acceleration of enthalpic relaxation. As these regions are more tightly packed it may be that the greater number of constrained amorphous chain segments contribute to localised relaxations which has the effect of accelerating physical ageing [51, 52]. Essentially because there are a greater number of possible molecular relaxations in the more tightly packed amorphous fraction over a given area compared to the free amorphous fraction, any segmental molecular mobility contributes a greater degree of enthalpic relaxation and makes the relaxation process more effective.

### 3.6 General Discussion

In support of previous work it was demonstrated that the rate at which a sample is cooled from a state of equilibrium to below  $T_g$  could influence the overall measured degree of enthalpic relaxation [19, 48]. In amorphous PEEK it was shown that for slower cooling rates it was possible to physically age the polymer on cooling. Therefore in order to cool through  $T_g$  without physically ageing the polymer, the amorphous fraction was reduced by introducing crystallinity and a constant cooling rate through  $T_g$  of 40°C was engineered into the sample prior to ageing.

It was then shown that an increasing degree of crystallinity reduced the degree of enthalpic relaxation for a given ageing temperature and time, as would be expected due to a reduced amorphous fraction. However due to difficulties in determining a significant trend between individual isothermally crystallised and non-isothermally crystallised data sets it was apparent that such an explanation is not satisfactory, and that the ageing characteristics were influenced by interactions at the crystal/amorphous interface [31, 34]. Due to the improved control offered by isothermal crystallisation when engineering a desired degree of crystallinity and crystalline morphology into a sample this method was subsequently adopted for conditioning.

A greater degree of crystallinity not only reduced enthalpy relaxation but was also shown to increase the breadth and measured position of the glass transition due to an increased restriction of the amorphous phase by the crystallites [32, 33]. This constraint of the amorphous fraction at the crystal interface required greater temperatures in order for chain segments to mobilise and depending on their proximity to the crystal face would introduce molecular motion at various temperatures, resulting in the broader transitions seen [24, 25].

This effect of crystallinity on the glass transition was further investigated by isothermally crystallising samples at high and low temperatures to develop a population of large but few, and small but numerous crystallites respectively [31, 49]. As the overall degree of crystallinity was kept constant it was therefore only the crystalline morphology affecting the transition region. It was found that cold crystallised samples further increased the glass transition temperature, due to thinner lamellae

increasing the crystal/amorphous interfacial area and therefore increasing the degree of constrained amorphous fraction. This can be assigned to the formation of crystallites in an environment of lower molecular mobility where chains are unable to transport to the growing crystal front and therefore become entangled and tethered to the crystal surface [29, 30].

As physical ageing is highly dependent upon the degree of undercooling from the glass transition it is essential the effect of crystalline morphology on  $T_g$  was taken into account when specifying the ageing temperature for a given polymer system [19]. Therefore samples of the same crystallinity, that had been cooled through  $T_g$  at a controlled rate, were all physically aged at  $10^\circ\text{C}$  below their measured thermodynamic glass transition temperature and the resulting enthalpic relaxation calculated. It was found that for a constant ageing time the cold crystallised samples relaxed to a greater degree, which initially seemed counterintuitive as the presence of a greater constrained amorphous fraction had been shown to restrict mobility. However it is this additional degree of constrained amorphous fraction which is thought to accelerate the physical ageing process [51, 52, 53].

As chains in this region are more tightly packed a greater number of chains are able to participate in the relaxation process when aged at temperatures approaching  $T_g$ , so more effective localised segmental mobility contributes to a greater degree of enthalpic relaxation [52]. This is because more amorphous chains are seen per unit area in the constrained region than in the free amorphous region.

Although mobility is restricted at the crystal/amorphous interphase which acts to raise  $T_g$ , as the ageing temperature is tailored to the  $T_g$  of the system, this effect of restriction is accounted for regardless of crystallisation temperature. The degree of crystallinity and consequently the amount of amorphous fraction present is also controlled between samples. Therefore as the cold crystallised samples form a greater constrained amorphous fraction on crystallisation [54], when ageing at a temperature where this restriction is accounted for, increased packing of amorphous regions at the crystal/amorphous interface accelerates the rate of enthalpic relaxation.

## Chapter 4 : Conclusions

---

- **Slow cooling through T<sub>g</sub> in amorphous PEEK introduces physical ageing**

Slow cooling through the glass transition region physically ages amorphous PEEK samples as they spend a greater period of time in close proximity to T<sub>g</sub> than those cooled at a faster rate [19, 48]. On subsequent ageing experiments the rate of enthalpic relaxation is reduced for slow cooled samples as they have already begun to relax, and on further approaching H<sub>∞</sub> the relaxation rate is continually reduced [19].

- **An increasing degree of crystallinity reduces enthalpic relaxation**

Samples of higher crystalline content were shown to relax to a lesser extent than those with a lower degree of crystallinity. This is due to a reduction in the degree of amorphous material present and also due to an increasing constraint on the amorphous fraction by crystallites [31, 32, 34].

- **An increasing degree of crystallinity raises the glass transition temperature**

For a greater degree of crystallinity the breadth and position of the glass transition temperature was shown to increase. Such an effect was caused by a reduction in mobility of the amorphous fraction at the crystal/amorphous interface, with amorphous chains closer to the crystal surface experiencing a greater degree of restriction [24, 25, 33].

- **For an equal degree of crystallinity reducing the isothermal crystallisation temperature acts to raise the glass transition temperature**

When degree of crystallinity was controlled, it was found that cold crystallised samples had a higher glass transition temperature. This is due to the formation of smaller crystals with more numerous lamellae [31, 49] and a greater constraint of the amorphous fraction at the crystal/amorphous interface [29, 30].

- **For an equal degree of crystallinity, when ageing at a temperature which accounts for the change in  $T_g$  with  $T_c$ , isothermally cold crystallised samples show a greater degree of enthalpic relaxation**

Due to the greater degree of constrained amorphous fraction, isothermally cold crystallised samples were able to relax to a greater degree over a given ageing time than melt crystallised samples.

Although this constrained amorphous fraction had been shown to restrict mobility, due to more tightly packed chain segments a greater number of segmental molecular relaxations are able to contribute to the process and ultimately accelerate physical ageing [51, 52, 53].

## Chapter 5 : Further Work

---

It is evident that further work is required in order to fully support the theory that for an equal crystallinity, a given ageing time and a controlled undercooling from the measured thermodynamic  $T_g$ , cold crystallised samples show more enthalpic relaxation due to a greater degree of constricted amorphous phase. However, due to the inherent lengthy nature of physical ageing studies it was not possible to conduct the full range of experiments desired.

For instance it would be interesting to find whether if left for long enough periods of time the cold crystallised and melt crystallised samples would fully relax (i.e reach  $H_\infty$ ) and show the same degree of enthalpic recovery on reheating. It is predicted that although the melt crystallised samples may take longer, as both samples have the same overall amorphous fraction eventually the enthalpy recovered on ageing after fully relaxing the samples would be equal. If not it may be the case that the constrained and free amorphous fractions may ultimately only be able to relax to certain degrees.

Such a finding would then require further work to probe the relative degrees of constrained and free amorphous fractions present in PEEK samples. For example if aged for periods of time long enough for samples to reach  $H_\infty$  it may be the case that although it takes longer, the melt crystallised samples are able to relax to a greater degree. This would suggest that although the constrained amorphous phase initially accelerates ageing, due to the restrictions imposed by the crystalline regions it cannot relax to the same degree as the free amorphous region.

Due to the variation in breadth of  $T_g$  with crystalline morphology it would also be interesting to investigate how tailoring the ageing temperature to different  $T_g$  measurements affects the results. For example measure the degree of undercooling from the onset of the transition, as opposed from the thermodynamic  $T_g$  as in this work. By varying the undercooling from various  $T_g$  measurements, it may be possible to determine whether the findings in this work are consistent. It may be seen that on



ageing at higher temperatures the results are accentuated as a greater degree of segmental mobility in the constrained amorphous phase could further accelerate relaxation and contribute to a larger enthalpic recovery peak.

## References

---

- 1) Attwood, T.E., Dawson, P.C., Freeman, J.L., Hoy, L.R.J., Rose, J.B. & Staniland, P.A. (1981) Synthesis and properties of polyaryletherketones. **Polymer**, 22: 1096-1103.
- 2) Dawson, P.C. & Blundell, D.J. (1980) X-ray data for poly(aryl ether ketones). **Polymer**, 21: 577-578.
- 3) Cheng, S.Z.D, Cao, M.-Y. & Wunderlich, B. (1986) Glass Transition and melting behaviour of Poly(oxy-1,4-phenyleneoxy-1,4-phenylenecarbonyl-1,4-phenylene). **Macromolecules**, 19: 1868-1876.
- 4) Cebe, P. & Hong, S.-D. (1986) Crystallisation behaviour of poly(ether-ether-ketone). **Polymer**, 27: 1183-1192.
- 5) Blundell, D.J. & Osborn, B.N. (1983) The morphology of poly(aryl-ether-ether-ketone). **Polymer**, 24: 953-958.
- 6) Blundell, D.J. (1987) On the interpretation of multiple melting peaks in poly(ether ether ketone). **Polymer**, 28: 2248-2251.
- 7) Bassett, D.C., Olley, R.H. & Al Raheil, I. (1988) On crystallisation phenomena in PEEK. **Polymer**, 29: 1745-1752
- 8) Olley, R.H., Bassett, D.C. & Blundell, D.J. (1986) Permanganic etching of PEEK. **Polymer**, 27: 344-348.
- 9) Hay, J.H., Kemmish, D.J. (1988) Environmental stress crack resistance of and absorption of low-molecular weight penetrants by poly(aryl ether ether ketone). **Polymer**, 29: 613-618.
- 10) Barton, J.M., Goodwin, A.A., Hay, J.N. & Lloyd, J.R. (1991) Absorption of low-molecular-weight penetrants by poly(aryl ether ketone): 2. Bromoform. **Polymer**, 32 (2): 261-264.
- 11) Lee, W.I., Talbot, M.F., Springer, G.S., Berglund, L.A. (1987) Effects of cooling rate on the crystallinity and mechanical properties of thermoplastic composites. **Journal of Reinforced Plastics and Composites**, 6: 2-12.
- 12) Cowie, J.M.G. (1991) **Polymers: chemistry and physics of modern materials**. 2<sup>nd</sup> ed. London: Blackie Academic & Professional.

- 13) Day, M., Deslandes, Y., Roovers, J. & Suprunchuk (1991) Effect of molecular weight on the crystallization behaviour of poly(aryl ether ether ketone): a differential scanning calorimetry study. **Polymer**, 32 (7): 1258-1266.
- 14) Wunderlich, B. (2005) **Thermal Analysis of Polymeric Materials**. Berlin: Springer.
- 15) Di Lorenzo, M.L. & Silvestre, C. (1999) Non-isothermal crystallisation of polymers. **Progress in Polymer Science**, 24: 917-950.
- 16) Gibbs, J.H. & Di Marzio, E. (1958) Nature of the glass transition and the glassy state. **The Journal of Chemical Physics**, 28 (3): 373-383.
- 17) Richardson, M.J. (1994) "The glass transition region". In: Mathot, V.B.F. (ed.) **Calorimetry and thermal analysis of polymers**. Munich: Hanser Publishers. pp: 169-188.
- 18) Holdsworth, P.J., & Turner-Jones, A. (1970) The melting behaviour of heat crystallized poly(ethylene terephthalate). **Polymer**, 12: 195-208.
- 19) Hutchinson, J.M. (1995) Physical ageing of Polymers. **Progress in Polymer Science**, 20: 703-760.
- 20) Cowie, J.M.G & Ferguson, R. (1993) Physical ageing of poly(methyl methacrylate) from enthalpy relaxation measurements. **Polymer**, 34 (10): 2135-2141.
- 21) Brunacci, A., Cowie, J.M.G., Ferguson, R. & McEwenm I.J. (1997) Enthalpy relaxation in glassy polystyrenes: 1. **Polymer**, 38 (4): 865-870.
- 22) Aref-Azar, A., Biddlestone, F., Hay, J.N. & Haward, R.N. (1983) The effect of physical ageing on the properties of poly(ethylene terephthalate). **Polymer**, 24: 1245-1251.
- 23) Kemmish, D.J. & Hay, J.N. (1985) The effect of physical ageing on the properties of amorphous PEEK. **Polymer**, 26: 905-912.
- 24) Struik, L.C.E (1987) The mechanical and physical ageing of semicrystalline polymers: 1. **Polymer**, 28: 1521-1533
- 25) Struik, L.C.E (1987) The mechanical behaviour and physical ageing of semicrystalline polymers: 2. **Polymer**, 28: 1534-1542.
- 26) Struik, L.C.E (1989) Mechanical behaviour and physical ageing of semi-crystalline polymers: 3. Prediction of long term creep from short time tests. **Polymer**, 30: 799-814.
- 27) Struik, L.C.E (1989) Mechanical behaviour and physical ageing of semi-crystalline polymers: 4. **Polymer**, 30: 815-830.
- 28) Ivanov, D.A., Legras, R. & Jonas, A.M. (1999) Interdependencies between the evolution of amorphous and crystalline regions during isothermal cold crystallization of poly(ether-ether-ketone). **Macromolecules**, 32: 1582-1592.
- 29) Righetti, M.C. & Tombari, E. (2011) Crystalline, mobile amorphous and rigid amorphous fractions in poly(L-lactic acid) by TMDSC. **Thermochimica Acta**, Article In Press.

- 30) Ma, Q., Georgiev, G. & Cebe, P. (2011) Constrains in semicrystalline polymers: Using quasi-isothermal analysis to investigate the mechanisms of formation and loss of the rigid amorphous fraction. **Polymer**, Article In Press.
- 31) Hay, J.N. (1995) The physical ageing of amorphous and crystalline polymers. **Pure & Applied Chemistry**, 67 (11): 1855-1858.
- 32) Atkinson, J.R., Hay, J.N. & Jenkins, M.J. (2002) Enthalpic relaxation in semi-crystalline PEEK. **Polymer**, 43: 731-735.
- 33) Mano, J.F., Gomez Ribelles, J.L., Alves, N.M. & Salmeron Sanchez, M. (2005) Glass transition dynamics and structural relaxation of PLLA studied by DSC: Influence of crystallinity. **Polymer**, 46: 8258-8265.
- 34) Vigier, G. & Tatibouet, J. (1993) Physical ageing of amorphous and semicrystalline poly(ethylene terephthalate). **Polymer**, 34 (20): 4257-4266.
- 35) Zhao, J., Wang, J., Li, C. & Fan, Q. (2002) Study of the amorphous phase in semicrystalline poly(ethylene terephthalate) via physical ageing. **Macromolecules**, 35: 3097-3103.
- 36) Hutchinson, J.M. & Kriesten, U. (1994) Physical aging and enthalpy relaxation in polypropylene. **Journal of Non-Crystalline Solids**, 172-174: 592-596.
- 37) Hone, G.W.H. (1994) "Fundamentals of differential scanning calorimetry and differential thermal analysis". In: Mathot, V.B.F. (ed.) **Calorimetry and thermal analysis of polymers**. Munich: Hanser Publishers. pp: 47-90.
- 38) Richardson, M.J. (1994) "DSC on polymers: Experimental conditions". In: Mathot, V.B.F. (ed.) **Calorimetry and thermal analysis of polymers**. Munich: Hanser Publishers. pp: 91-104.
- 39) Richardson, M.J. (1997) Quantitative aspects of differential scanning calorimetry. **Thermochimica Acta**, 300: 15-28.
- 40) Hutchinson, J.M., Ruddy, M. & Wilson, M. R. (1988) Differential scanning calorimetry of polymer glasses: corrections for thermal lag. **Polymer**, 29: 152-159
- 41) Gray, A.P. (1970) Polymer crystallinity determinations by dsc. **Thermochimica Acta**, 1: 563-579.
- 42) Blundell, D.J., Beckett, D.R. & Wilcocks, P.H. (1981) Routine crystallinity measurements of polymers by d.s.c. **Polymer**, 22: 704-707.
- 43) Kong, Y. & Hay, J.N. (2002) The measurement of the crystallinity of polymers by DSC. **Polymer**, 43: 3873-3878.
- 44) Kong, Y. & Hay J.N. (2003) The enthalpy of fusion and degree of crystallinity of polymers as measured by DSC. **European Polymer Journal**, 39: 1721-1727.
- 45) Richardson, M.J. & Savill, G.N. (1975) Derivation of accurate glass transition temperatures by differential scanning calorimetry. **Polymer**, 16: 753-757.

- 46) Aras, L. & Richardson, M.J. (1989) The glass transition behaviour and thermodynamic properties of amorphous polystyrene. **Polymer**, 30: 2246-2252.
- 47) Hutchinson, J.M. (2009) Determination of the glass transition temperature. **Journal of Thermal Analysis and Calorimetry**, 98: 579-589.
- 48) Surana, R., Pyne, A., Rani, M. & Suryanarayanan, R. (2005) Measurement of enthalpic relaxation by differential scanning calorimetry – effect of experimental conditions. **Thermochimica Acta**, 433: 173-182.
- 49) Aref-Azar-A., Arnoux, F., Biddlestone, F. & Hay, J.N. (1996) Physical ageing in amorphous and crystalline polymers. Part 2. Polyethylene terephthalate. **Thermochimica Acta**, 273: 217-229.
- 50) Krishnaswamy, R.K. & Kalika, D.S. (1994) Dynamic mechanical relaxation properties of poly(ether ether ketone). **Polymer**, 35 (6): 1157-1165.
- 51) Krishnaswamy, R.K., Geibel, J.F. & Lewis, B.J. (2003) Influence of semicrystalline morphology on the physical ageing characteristics of poly(phenylene sulfide). **Macromolecules**, 36: 2907-2914.
- 52) Shelby, M.D. & Wilkes, G.L. (1998) Thermodynamic characterization of the oriented state of bisphenol A polycarbonate as it pertains to enhanced physical ageing. **Journal of Polymer Science: Part B: Polymer Physics**, 36: 2111-2128.
- 53) Shelby, M.D. & Wilkes, G.L. (1998) The effect of molecular orientation on the physical ageing of amorphous polymers – dilatometric and mechanical creep behaviour. **Polymer**, 39 (26): 6767-6779.
- 54) Huo, P & Cebe, P. (1992) Temperature-dependent relaxation of the crystal-amorphous interphase in poly(ether ether ketone). **Macromolecules**, 25: 902-905.

## Appendix I: Baseline Subtraction

---

Due to the wide temperature range over which PEEK crystals melt it is important to establish a consistent method of measuring the heat of fusion on melting so an accurate degree of crystallinity can be determined. As discussed in the introduction a number of authors have suggested subtracting a baseline in order to remove the influence of any slope and curvature inherent to DSC.

When investigating whether or not it was necessary to subtract a baseline from the traces recorded in this work, the effect of heating rate was also probed in order to determine a suitable scanning rate which was a compromise between the melting and recrystallisation of crystallites observed at slow scanning rates with that of thermal lag seen at fast scanning rates.

In order to subtract a baseline prior to the sample being crystallised a trace had to be obtained for the empty sample pan. Scans were recorded for empty pans and lids at 5, 10, 20, 40, 50, 60, 80, 100, 160°C/min from 80 – 400°C and then cooled back to room temperature. The pans were filled and the lids put back on before the individual polymer sample was heated to the melt and crystallised at 40°C/min to give a standard crystallinity across samples ( $31 \pm 0.5\%$ ). When back at room temperature the filled pans were then scanned to the melt at the same rate they had been when previously unfilled and the traces recorded.

As shown in Figure I there was very little difference between the baseline subtracted and un-subtracted traces, and on measuring parameters for the heat of fusion of the melting peak the data sets were found to be highly consistent. Therefore due to the accuracy of this calorimeter and low intrinsic slope and curvature over the temperature region of interest it was deemed unnecessary to record an empty pan and lid baseline prior to each data set for subsequent investigations.

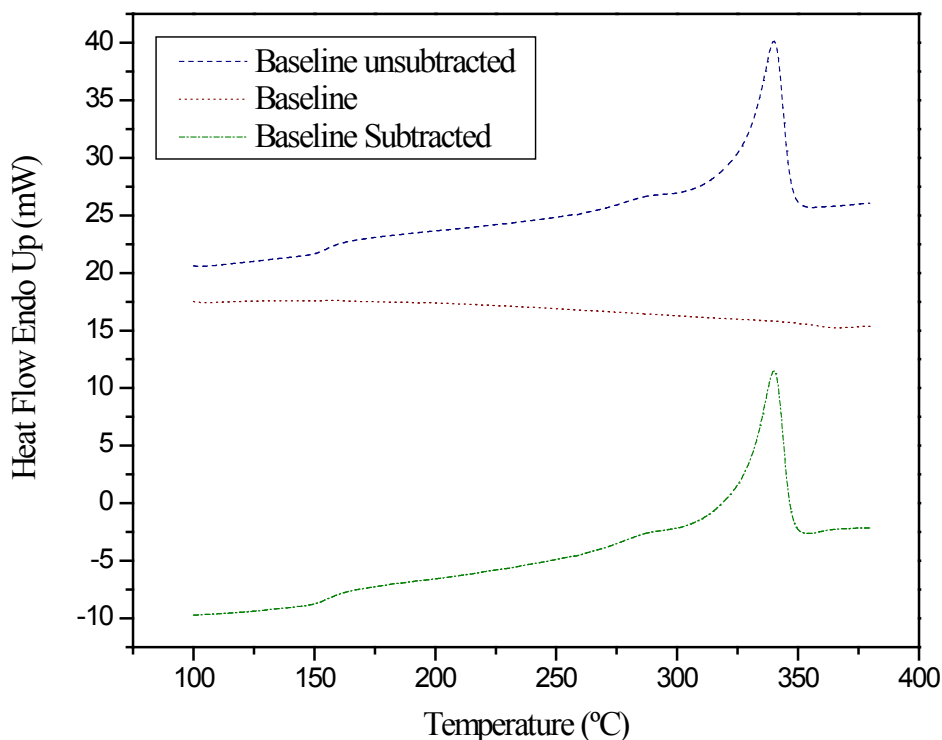


Figure I. The effect of baseline subtraction on a sample scanned to the melt at 80°C/min.

Of rather more importance to this work was the selection of an appropriate scanning rate to minimise the influence of recrystallisation and thermal lag. Samples of an equal degree of crystallinity were scanned at the various rates outlined above and two thermodynamic points were selected for comparison, as shown in Figure II these were the peak melt and the last trace of crystallinity. It can be seen that for slow heating rates ( $< 20^{\circ}\text{C}/\text{min}$ ) the last trace and peak melt are pushed to higher temperatures due to the recrystallisation phenomenon, and for faster heating rates ( $> 60^{\circ}\text{C}/\text{min}$ ) are pushed upwards due to thermal lag. Therefore an intermediate temperature of  $40^{\circ}\text{C}/\text{min}$  shall be used in this work as it allows scanning from  $80 - 400^{\circ}\text{C}$  to be completed in an experimentally acceptable time frame and minimises the influence of recrystallisation and thermal lag. Figure II also supports the conclusion that a baseline need not be subtracted in this work as the measured data points are in very good agreement.

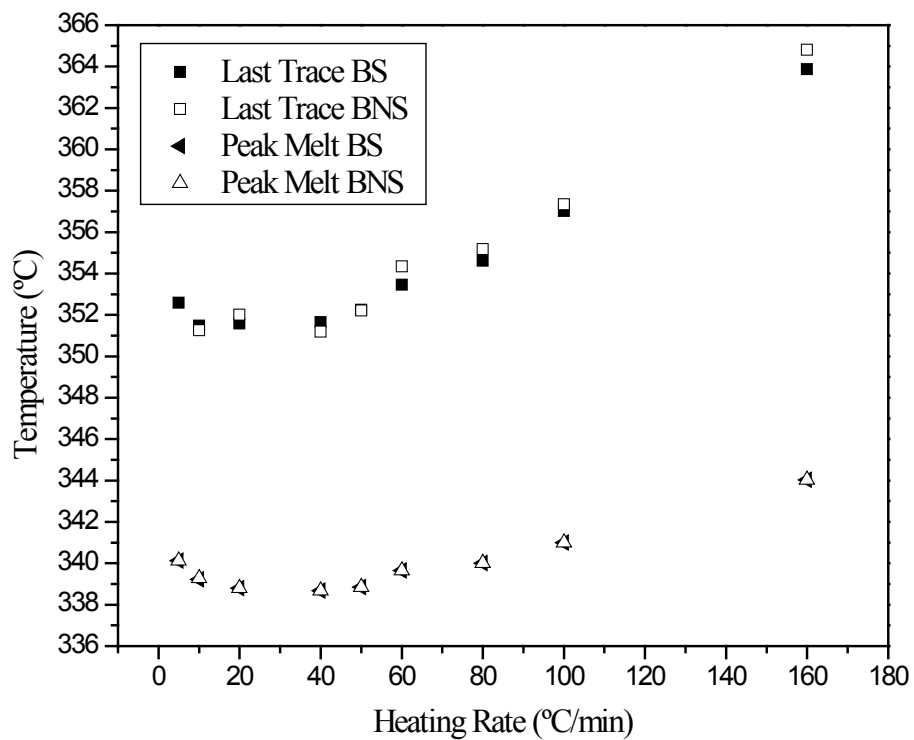


Figure II. The influence of heating rate on the measured values for last trace of crystallinity and peak melting temperatures for samples of equal crystallinity. The effect of subtracting a baseline on the measured values is also plotted. BS: Baseline Subtracted / BNS: Baseline Not Subtracted



## Appendix II: Formation of Additional Crystallinity on Cooling and Reheating

---

When engineering a desired morphology into a polymer at a certain isothermal temperature for a given time it is important that the degree of crystallinity developed in the sample is sufficient to prevent any further crystallisation on cooling or reheating. If additional crystallinity is introduced the crystal morphology will no longer be representative of that developed at  $T_c$  and the range of crystal entities may lead to anomalous results even if the overall degree of crystallinity is kept constant.

The development of additional crystallinity on cooling can be seen in Figure III.a where samples were isothermally crystallised at 312°C for 2, 4, 6, 10, 20 minutes and then cooled at 40°C/min to room temperature. It can be seen that on cooling from the melt to 312°C no crystallinity is introduced into the system prior to reaching  $T_c$  due to the rapid cooling rate of 160°C/min. On subsequent cooling from 312°C it is evident that for shorter crystallisation times the crystallisation exotherm is increasingly pronounced whereas for longer crystallisation times no such exotherm is observed, demonstrating that if sufficient crystallinity is not developed at  $T_c$  then additional crystallinity is able to form on cooling.

The subsequent re-heating traces are shown in Figure III.b and the most prominent feature is the development of a second endotherm on the main melting peak with increasing crystallisation time. When held at  $T_c$  for 2 minutes most, if not all, of the melting peak is that of crystallinity developed on cooling. However as you hold for longer periods of time, for a  $t_c > 4$  mins, less crystallinity is introduced on cooling and the melting peak is pushed to increasingly higher temperatures with the emergence of a minor endothermic peak. Should the dual lamellae model of primary and secondary crystallisation be applied, this indicates that much of the primary crystallisation is nearing a degree of completion and some secondary crystallisation is taking place – although not complete as further

crystallisation is still observed on cooling. For crystallisation times  $> 10$  mins crystallisation is no longer observed on cooling and the lower temperature, secondary crystallisation peak is far more pronounced. On cooling to below  $T_g$  this is representative of the desired morphology introduced at the isothermal crystallisation temperature as the degree of crystallinity is sufficient to prevent any additional crystallites forming over the intermediate temperature range.

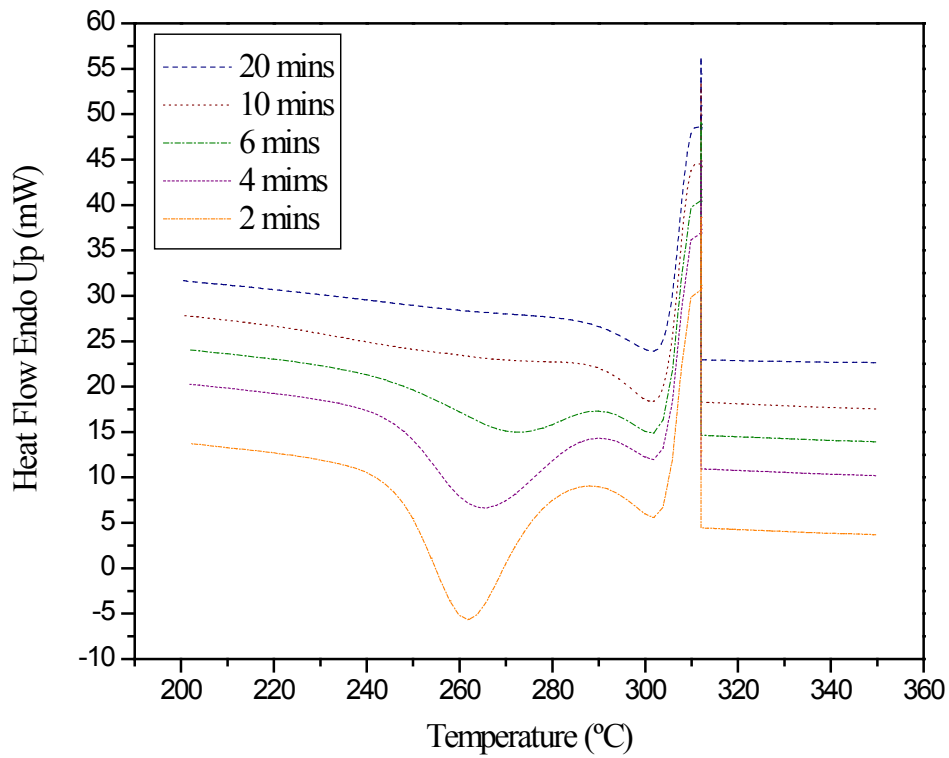


Figure III.a. The development of crystallinity on cooling at 40°C/min after crystallising samples at 312°C for various lengths of time.

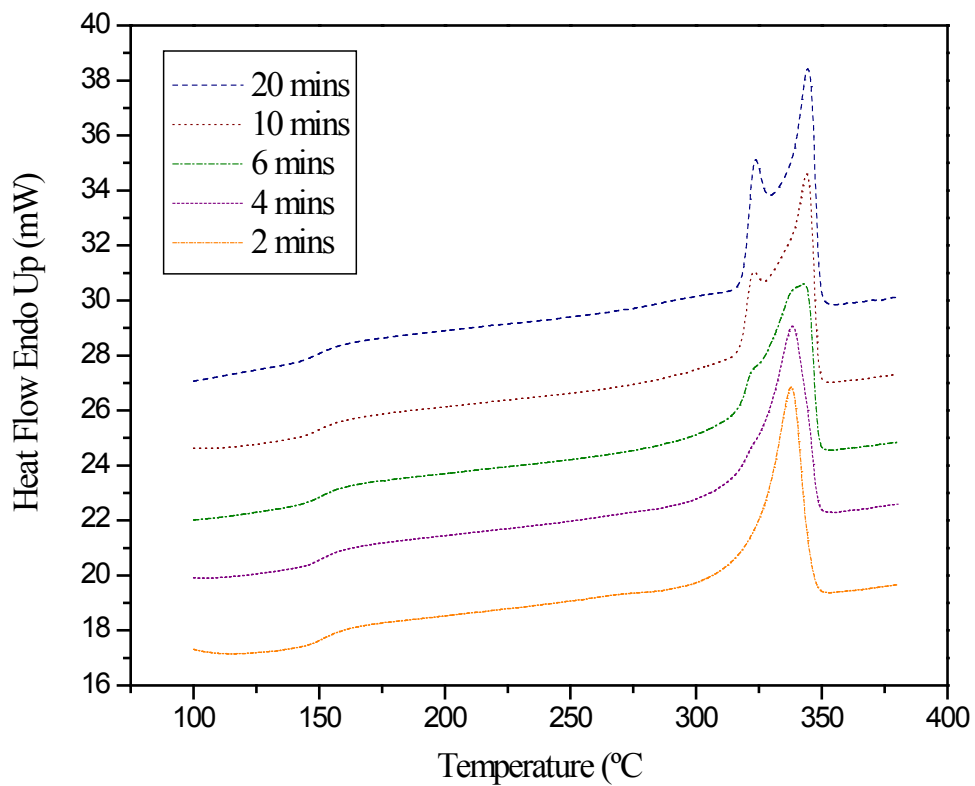


Figure III.b. Melting traces of the above samples crystallised at 312°C for differing lengths of time and then cooled to below  $T_g$  at 40°C/min. The melting trace is scanned at 40°C/min.

The same crystallisation exotherms can also be observed on heating samples which have been quenched from  $T_c$  after holding for various lengths of time and then scanning them into the melt. As before samples were isothermally crystallised at  $312^\circ\text{C}$  for 2, 4, 6, 10, 20 minutes but were then quenched directly into liquid nitrogen before scanning from  $80 - 400^\circ\text{C}$  at  $40^\circ\text{C}/\text{min}$  to obtain the melting traces, displayed in Figure IV. As previously observed on cooling, when scanning the quenched samples into the melt a decreasing crystallisation exotherm is produced in samples which have been held for increasingly longer times at  $T_c$ . Again the secondary endotherm appears with prolonged times at  $T_c$ , suggesting the development of secondary crystallites occurs once primary crystallisation has taken place. In order to measure the degree of crystallinity introduced for shorter crystallisation times the area of the exothermic crystallisation peak was subtracted from the heat of fusion of the endothermic melting peak, thus giving the degree of crystallinity prior to scanning and the development of any additional crystallinity forming on heating into the melt.

This is an overview of the preliminary work done which was essential in determining adequate isothermal crystallisation temperatures and times that would allow a desired morphology to be engineered into the polymer for subsequent ageing investigations.

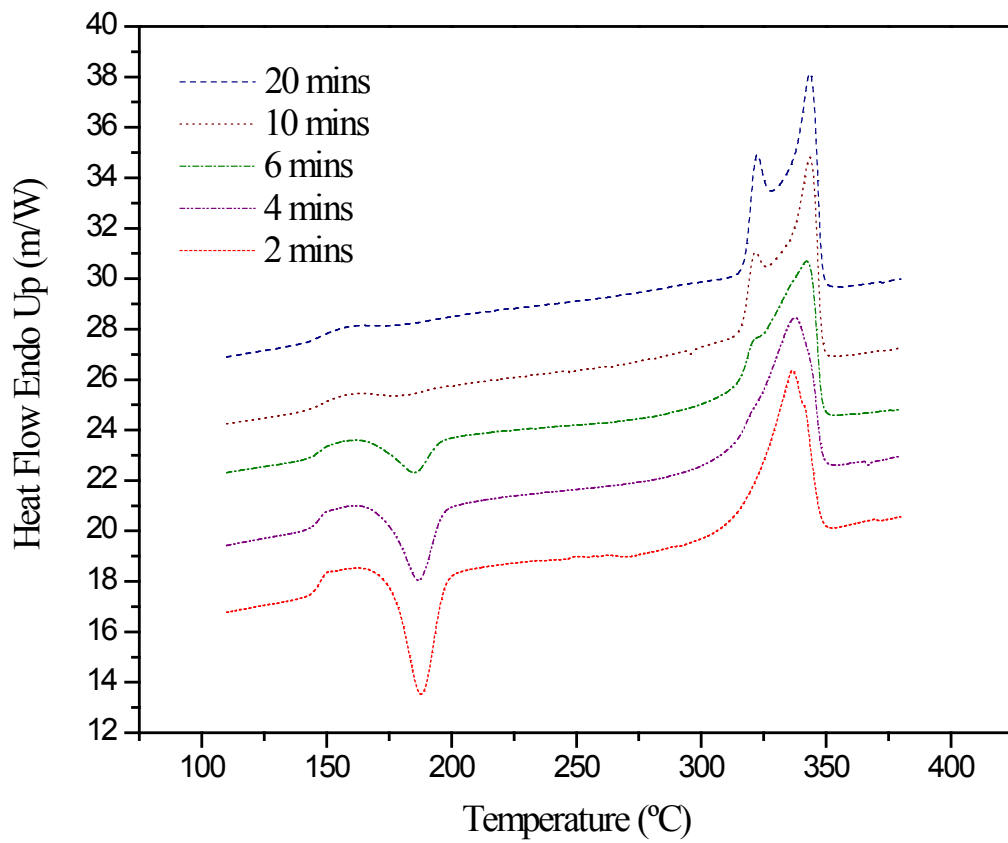


Figure IV. The 40°C/min heating scans of samples crystallised at 312°C for differing lengths of time and quenched to below T<sub>g</sub>.